Pergamon

Journal of Structural Geology, Vol. 16, No. 7, pp. 899 to 918, 1994

0191-8141/94 $07.00+0.00

Extensional origin of ductile fabrics in the Schist Belt, Central Brooks Range, Alaska—I. Geologic and structural studies

TIMOTHY A. LITTLE* and ELIZABETH L. MILLER

Geology Department, Stanford University, Stanford, CA 94305, U.S.A.

JEFFREY LEE†

Department of Earth Sciences, Monash University, Clayton, Victoria 3168, Australia

and

RICHARD D. LAW

Department of Geological Sciences, Virginia Polytechnic Institute and State University, Blacksburg, VA 24061, U.S.A.

(*Received* 6 *May* 1992; *accepted in revised form* 13 *September* 1993)

Abstract—Blueschist-facies rocks are locally preserved in the internal zone of the Brooks Range orogen, where a high-strain foliation (S_2) and down-dip stretching lineation occur for hundreds of kilometers along strike of the normal fault-bounded, southern edge of the orogen. This locally mylonitic fabric is inferred to represent an XY finite strain ratio of >30. The foliation formed during greenschist-facies overprinting of the blueschists and has been interpreted in different ways by geologists who disagree about the mechanism by which the high-P rocks were exhumed. Metamorphic fabrics and structures were studied in detail in the south-central Brooks Range, where the Florence Creek fault separates a hangingwall of weakly metamorphosed sedimentary rocks from high-P rocks of the Brooks Range Schist Belt. This fault may have in part pre-dated the D_2 overprint, as mylonitic fabrics are imprinted across both sides of the structure. The mylonites occur near the top of a ductile shear zone >8 km thick, and contain oblique-grain shape fabrics, shear bands and asymmetric quartz petrofabrics indicative of top-down-to-the-south (normal) shear. D_2 fabrics in quartzose schists are mylonitic and asymmetric at high structural levels of the footwall but are increasingly granoblastic and symmetric at deeper levels, suggesting increasing operation of temperature-sensitive recovery processes and a larger irrotational component of deformation with structural depth. D_2 strain decreases markedly about 10 km north of the fault zone, so that the earlier foliation is no longer transposed into S_2, and relict M_1 minerals (garnet, chloritoid) are preserved.

Our data suggest that high-strain tectonites along the southern margin of the Schist Belt did not form during contractional deformation in the Brooks Range orogen, but during mid-Cretaceous crustal extension, which was superimposed on previously thickened continental crust of the northernmost Cordillera. Temperatures may have increased during the later stages of extension in the southern Brooks Range and adjacent Yukon–Koyukuk basin region in concert with mid- to Late Cretaceous magmatism, allowing deformation and metamorphism of earlier-formed normal faults. Subsequent folding in the latest Cretaceous or Early Tertiary resulted in further exhumation of the schists and modified the geometry of the faults by large-scale folding.

INTRODUCTION

EXTENSIONAL deformation has now been shown to play an important but imperfectly understood role in the evolution of many orogenic belts (e.g. Dewey 1988). In particular, the degree to which extension is responsible for the exhumation of high-pressure metamorphic belts remains a controversial topic (see, for example, Hsu 1992, Platt 1992) and disagreement exists concerning the specific structural setting of such extension. Does extension occur synchronously with crustal thickening, as in the Himalayas (e.g. Burchfiel *et al.* 1992), or does it post-date crustal thickening as in the Basin and Range province of the western United States? Does extensional deformation represent localized gravitational 'collapse' of overthickened crust and high topography (e.g. Dewey 1988), or does it attenuate the entire lithosphere (e.g. McKenzie 1978)? In complexly deformed metamorphic rocks, which are commonly the main constituents of the internal zones of orogenic belts, the debate is fuelled by difficulties in distinguishing shortening from extension-related deformational fabrics. These issues are now being intensely debated in the Brooks Range, northern Alaska, where geologic relationships have only recently been scrutinized in light of the possible role of extensional tectonism (e.g. Gottschalk 1990, Miller & Hudson 1991, Miller & Hudson 1993, Till *et al.* 1993). In this paper, and the companion paper that follows it, we present new structural data from the internal zone of the central Brooks Range which bear on the issue of distinguishing and interpreting structural fabrics formed during differing tectonic regimes and discuss their impli-

*Current address: Department of Geology, Victoria University of Wellington, P.O. Box 600, Wellington, New Zealand.

†Current address: Division of Geological Sciences, California Institute of Technology, Pasadena, CA 91125, U.S.A.

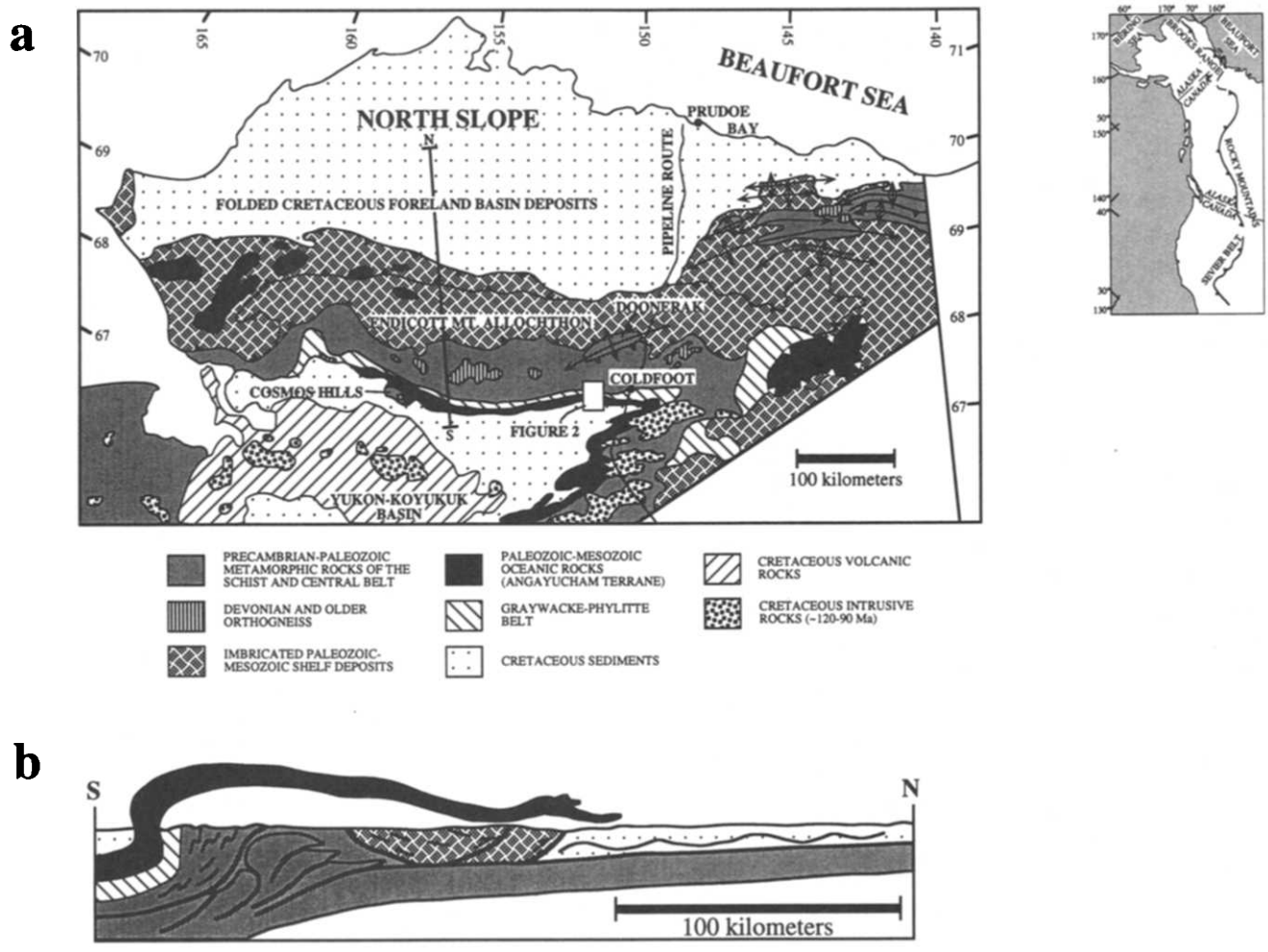

Fig. 1. (a) Index map and simplified tectonic map of the Brooks Range, showing location of study area. (b) Simplified and schematic tectonic cross-section of the Brooks Range at about latitude 155°W after Roeder & Mull (1978).

cations for the role of extensional deformation and the uplift of high pressure metamorphic rocks in this orogenic belt.

The Brooks Range, Arctic Alaska, represents the northwesternmost continuation of the Mesozoic–early Cenozoic foreland fold and thrust belt of the North American Cordillera (Fig. 1a). Although much of the stratigraphy and structure of the Brooks Range is continuous with that in the Canadian Cordillera, its geologic evolution is, by comparison, still poorly known. Exploration for oil and gas on the North Slope of Alaska has resulted in detailed studies that focus on the stratigraphy and structural history of the foreland-basin, and on the geometry of thin-skinned thrust faults in the northern foothills of the Brooks Range. N-directed thrust faulting in the Brooks Range is interpreted to have resulted in 500–800 km shortening of a Paleozoic to Early Jurassic continental shelf sequence (Oldow *et al.* 1987, Mayfield *et al.* 1988, Grantz *et al.* 1991) since Middle Jurassic time (Wilber *et al.* 1987, Mayfield *et al.* 1988). The earliest and structurally highest thrust faults carry obducted mafic–ultramafic igneous rocks and deep-water sedimentary rocks onto the shelf, closing an ocean basin that lay to the south (e.g. Roeder & Mull 1978). These oceanic rocks are represented by the Misheguk Mountain allochthon and related rocks of the Angayucham Terrane (Silberling & Jones 1984) (Fig. 1a). Following obduction, the underlying shelf sequence was imbricated northwards. The cessation of this period of thrusting is bracketed between the youngest strata involved, of Valanginian age (~130 Ma) and Aptian(?)–Albian strata (~115–110 Ma) that unconformably overlie deformed allochthons (see summary in Grantz *et al.* 1991). Foreland-basin sediments record renewed shortening beginning in the Late Cretaceous–Early Tertiary and continuing to the present day.

Southward within the Brooks Range, rocks become more metamorphosed and represent deeper structural levels of exposure (Grybeck *et al.* 1977, Mull 1982, Oldow *et al.* 1987). Here the correlation of rock units, the geometry and displacement of major faults, and the timing of events are less well understood. Metamorphic rocks exposed in the southernmost part of the range, which are thought to represent the most deeply exhumed structural levels of the orogen, consist of metasedimentary and metaigneous rocks of late Proterozoic to Devonian age which probably formed depositional basement for the Paleozoic–Mesozoic shelf sequences imbricated into the northern part of the thrust belt (e.g. Dillon *et al.* 1980, Armstrong *et al.* 1986, Mull *et al.* 1987). Rocks of the 'Schist Belt' along the southern margin of the Brooks Range have attracted particular

attention because of the occurrence of blueschists and locally, eclogite (e.g. Hitzman *et al.* 1986, Gottschalk & Oldow 1988, Till *et al.* 1988, Dusel-Bacon *et al.* 1989). Most workers regard the blueschists as having developed during Jura-Cretaceous thrusting, which involved obduction of the oceanic allochthon and imbrication and thickening of underlying continental margin. The system of S-dipping faults that overlie the Schist Belt and bound the Angayucham terrane along the southernmost flank of the Brooks Range has, in turn, been traditionally interpreted as an Alpine-style root zone (e.g. Mull *et al.* 1987, Dillon 1989) (Fig. 1b) and the fabrics developed beneath these faults have been linked to the same crustal thickening event. Several recent studies question these earlier interpretations, suggesting that this fault system may have normal rather than thrust displacement (Box 1987, Miller 1987, Gottschalk 1987, Gottschalk & Oldow 1988, Ave Lallement *et al.* 1989, Christiansen 1989, Miller *et al.* 1990a,b), but most workers ascribe all penetrative ductile fabrics in the structurally underlying Schist Belt to crustal shortening (Gottschalk 1990, Patrick *et al.* 1991, Oldow *et al.* 1991, Till & Moore 1991, Till *et al.* 1993).

This paper presents the results of detailed geologic mapping and structural studies in the Schist Belt in the Wiseman quadrangle, southern Brooks Range (Figs. 1 and 2), an area previously mapped in reconnaissance by Dillon *et al.* (1981, 1986). In this area the Schist Belt contains two foliations, an older one that developed during high-*P* metamorphism, and a younger one that formed during a greenschist-facies overprint (Dillon *et al.* 1981, 1986). The study was carried out to better characterize the deformational history of metamorphic tectonites beneath the inferred normal fault system. These new data suggest that extensional overprinting of earlier formed blueschist-facies metamorphic fabrics are far more pervasive than previously thought, and that most of the measurable ductile strain in these rocks is a consequence of N–S-stretching in conjunction with top-down-to-the-south extensional shear. Fabrics of similar nature and with similar orientation in other areas of study have been interpreted as thrust-related, underscoring the controversial nature of the results reported in this paper.

GEOLOGICAL AND STRUCTURAL FRAMEWORK

The southern Brooks Range consists of a series of S-dipping metamorphic units that are progressively less metamorphosed to the south (Fig. 1a). The nature of contacts between units is not clear-cut, in part because some contacts are strongly deformed and metamorphosed. The southernmost of these units, the Angayucham terrane, consists of metabasalt and lesser radiolarian chert and pelagic limestone of Devonian to Jurassic age (Bird 1977, Jones *et al.* 1988) metamorphosed in the prehnite–pumpellyite facies (e.g. Dusel-Bacon *et al.* 1989). A thick section of Cretaceous (Albian–Aptian) conglomerate and sandstone unconformably overlie these oceanic rocks along the northern flank of the Yukon–Koyukuk depression (Dillon 1989) (Fig. 1a). To the north, the Angayucham terrane lies in fault contact above a thin panel of very low-grade metagraywacke and lesser phyllite that in several localities along strike has yielded Devonian palynomorphs (Gottschalk 1987, Murphy & Patton 1988). This poorly exposed metagraywacke–phyllite (MP) unit can be subdivided into two regionally mappable subunits, a southern unit consisting chiefly of weakly deformed metagraywacke and a northern unit of strongly deformed phyllite (Brosge & Reiser 1964, Dillon *et al.* 1986). Gottschalk & Oldow (1988) report that the phyllite unit near Coldfoot was metamorphosed in the pumpellyite–actinolite facies.

Structurally beneath and to the north of the MP unit, the Brooks Range Schist Belt consists of pelitic and quartzose schists, lesser amounts of mafic to silicic metavolcanic rocks, calcareous schists or marble, and minor deformed granitoids (e.g. Brosge & Reiser 1971, Nelson & Grybeck 1980, Dillon *et al.* 1986). Based on sparse fossils, mostly of Devonian age, and U–Pb determinations on zircon, rocks of the Schist Belt are thought to range in age from late Proterozoic to Late Devonian (e.g. Dillon *et al.* 1980, Hitzman *et al.* 1986, Armstrong *et al.* 1986). Mafic schists containing epidote + glaucophane–crossite ± garnet and pelitic schists preserving the assemblage glaucophane + chloritoid + garnet occur widely but discontinuously within the Schist Belt (see references in Dusel-Bacon *et al.* 1989). Pseudomorphs after lawsonite have been reported locally (Till *et al.* 1988). Although these high-*P*–low-*T* assemblages may once have been pervasive in the Schist Belt, in most areas they have been retrogressed during later greenschist-facies metamorphism (Dusel-Bacon *et al.* 1989). In the central Brooks Range, the contact between the MP unit and the Schist Belt has been interpreted as a brittle normal fault (e.g. Gottschalk & Oldow 1988, Dillon 1989). In our area of study, ductile deformation and metamorphism overprint and obscure this contact. The Schist Belt is structurally overlain to the north by a sequence of metamorphic rocks referred to as the 'central belt', the Hammond Terrane or the Skajit allochthon, but not all workers agree as to the location, nature and geometry of this contact. Figure 1(a) shows the interpretation of Moore *et al.* (1992) in which the Hammond terrane overlies the Schist Belt, but see Oldow *et al.* (1987) for the opposite interpretation. Still farther north, the Endicott Mountains allochthon (Fig. 1a) contains relatively unmetamorphosed sedimentary rocks of Paleozoic–Mesozoic age (Mull 1982, Oldow *et al.* 1987, Handschy 1988).

STRUCTURAL GEOLOGY OF THE FLORENCE–FALL CREEKS REGION

Most of the units introduced above occur in our detailed study area (Figs. 2 and 3). Their lithology, metamorphic grade and style of deformation are briefly

summarized below. In the southernmost part of the study area, massive amygdaloidal metabasalt of the Angayucham Terrane has well-preserved primary igneous textures, and interbedded cherts contain Late Mississippian–Early Pennsylvanian radiolaria (Dillon *et al.* 1981). Immediately south of the map area, a poorly exposed conglomerate-rich sequence of Cretaceous clastic rocks several kilometers thick is inferred to depositionally overlie metabasalt along a marked angular unconformity (Dillon *et al.* 1981). An unexposed S-dipping fault, here termed the Angayucham Fault, separates Angayucham metabasalt from the structurally underlying MP unit (Fig. 2). This fault zone is inferred to be equivalent to the Angayucham 'thrust' system of Dillon *et al.* (1986) and the Cathedral Mountain fault zone of Gottschalk & Oldow (1988) farther east. The metagraywacke subunit of the MP unit consists chiefly of tightly folded and cleaved, lithic-bearing quartzose metasandstone interbedded with minor metasiltstone and slate or phyllite. Relict sedimentary structures include bedding, parallel laminations and grading. A second poorly exposed contact separates the metagraywacke unit (Dqp, Fig. 2) from the structurally underlying phyllite subunit (Dpq), which is characterized by a greater abundance of dark grey phyllite and lesser thin beds of metagraywacke. Interlayering of the two lithologies in both subunits, and their similarity in detrital petrography, metamorphic grade and structural fabrics suggests that the contact between the two subunits may be stratigraphic.

A S-dipping zone of increased deformation, interpreted as a shear zone, separates the phyllite subunit from structurally underlying, locally mylonitic, rocks of the Schist Belt (Figs. 2 and 4, A–A′). This shear zone is expressed by higher strains in both the phyllite subunit and the Schist Belt as the contact is approached. This contact is here termed the Florence Creek Fault (FCF), a ~10 m wide zone that dips about 40–50°S and locally includes what appear to be fault-bound slivers of exotic lithologies including quartzite, marble, quartzofeldspathic orthogneiss(?) and garnet-stilpnomelane bearing mafic schist. Rocks within, and on either side of the FCF share the last major regional deformational event, which was associated with development of a strong foliation throughout most of the map area, and, as discussed above, the intensified strain developed adjacent to the fault itself (S_d in the MP unit, S_2 in Schist Belt).

Upper parts of the Schist Belt in the study area consist chiefly of pelitic schist and subordinate metaquartzite (unit Pzqms in Figs. 2 and 3). Pelitic quartz–mica schist is locally interlayered with black graphitic schist (Pzgs), lenticular bodies (probably deformed dykes or sills) up to 20 m thick of mafic schist and metagabbro (Pzg and Pzgm), and several meter-thick bodies of meta-andesite and meta-rhyolite (Pzca), some of which preserve pyroclastic textures. Meter-thick units of impure marble locally occur adjacent to metavolcanic layers. Taken together, this assemblage composes what is here informally referred to as the quartz–mica schist-rich (QMS) unit. The QMS unit overlies an assemblage of thickly interlayered impure calcschist (Pzcs), graphitic marble (Pzbm), pure marble (Pzsm) and minor pelitic schist (Pzqms). This contact dips south and is concordant with, or transposed into parallelism with, the dominant foliation in the Schist Belt, S_2 (Fig. 4, B–B′). The structurally deeper assemblage is here referred to informally as the calc-schist-rich (CS) unit.

Metagraywacke–phyllite unit

Rocks in the MP unit preserve detrital textures and are cut by a well-developed foliation, which we call S_d, for dominant foliation (Fig. 5a). S_d is axial planar to mesoscopic folds of bedding. F_d folds are close to isoclinal, with angular to rounded hinges, and have wavelengths from 4 cm up to at least 2 m. Bedding and the S_d cleavage generally dip moderately to the south (Figs. 7a & b). Fold hinges plunge south, nearly down the dip of S_d, and are commonly strongly undulatory, but were nowhere observed to be sheath folds. The intersection of this cleavage with bedding or early quartz veins defines a lineation (Fig. 7a).

In pelitic rocks, S_d is a domainal slaty cleavage defined by alignment of micaceous films and trails of graphitic dust concentrated along pressure solution seams. In metagraywacke, S_d is a rough cleavage defined by flattened detrital quartz grains, anastomosing films of white mica and chlorite, and fibrous beards of white mica and quartz. Truncation of spindle-shaped quartz grains by discrete cleavage seams of micaceous and graphitic residue indicates that diffusive mass transfer was an important deformation mechanism (Fig. 5b). Crystal-plastic deformation and dynamic recrystallization of quartz were additional deformation mechanisms, as indicated by undulatory extinction and subgrain development in detrital grains, and local development of finely recrystallized asymmetric trails or 'mortar texture' on the rims of such grains. Although S_d is the only foliation consistently observed throughout the MP unit, some rocks in the phyllite subunit contain an earlier cleavage, subparallel to bedding, that is crenulated by S_d.

The strain gradient towards the FCF is expressed by a transition in metagraywacke textural zones (Bishop 1972) from zone 1 in the southern metagraywacke subunit to zone 3b in schists adjacent to the FCF (Fig. 4, A–A′). In pelitic rocks, S_d is a fine-grained slaty cleavage in the southern parts of the metagraywacke subunit, but becomes progressively more coarse-grained and phyllitic to the north. In metagraywacke biotite occurs as a kinked detrital mineral; however, in some samples of flaggy psammitic schist adjacent to the FCF, flakes of fine-grained biotite aligned with S_d are of probable metamorphic origin. The most strongly deformed metagraywackes occur adjacent to the FCF. These flaggy mylonitic schists contain a down-dip stretching lineation, L_{de}, defined by ribbon-shaped, relict detrital quartz grains (Figs. 5b and 7b). These relationships suggest that not only strain intensity but also peak

metamorphic temperatures during deformation increase structurally downwards towards the FCF.

Shear-sense indicators in more highly strained rocks include oblique grain-shape foliations defined by dynamically recrystallized quartz grains, asymmetric recrystallized tails on quartz porphyroclasts, and diffuse crossed girdle quartz *c*-axis petrofabric patterns with an asymmetric density distribution (Fig. 7) (Law *et al.* 1994). Near the FCF, late-stage ductile shear bands (extensional crenulation cleavage of Platt & Vissers 1980) cut and deflect S_d (Fig. 5c). With only a few exceptions, these late-stage shear bands indicate a top-down-to-the-south sense of shear (Fig. 7).

Quartz–mica schist-rich unit of the Schist Belt

The QMS unit that structurally underlies the phyllite unit beneath the FCF consists of recrystallized, medium-grained schists that lack any vestige of detrital texture. The schists are polydeformed, commonly retaining evidence for at least one schistosity (S_1) that predates the dominant S-dipping foliation, S_2. Where D_2 strain is lower, compositional layering in the schists is subparallel to S_1, a domainal foliation defined by thin quartzose laminations, micaceous folia, and quartz veinlets. This foliation is everywhere plicated by tight to isoclinal crenulations, and transposed into parallelism with S_2. In the most strongly deformed rocks only the younger foliation, S_2 is evident. We use conventional subscript nomenclature for these two foliations because they have a consistent temporal and geometric relationship to one another throughout the study area and are believed to have developed at a high angle to one another. Use of the 'transposition cycle' nomenclature (e.g. Tobish & Paterson 1988), used by previous workers in the Brooks Range (Gottschalk 1990, Patrick *et al.* in press) provides no additional descriptive information and carries with it the genetic implication of a progressive deformational history.

F_2 crenulations have half-wavelengths up to the maximum spacing of S_2 cleavage, about 1.5 cm, but are generally more narrowly spaced. Mesoscopic folds of S_1, with half-wavelengths up to ~20 cm, approximate a class 2 (similar) fold geometry. S_2 is axial planar to these folds, dips moderately to the south, and is subparallel to S_d in the MP unit (Fig. 7d). S_2 can be traced structurally upward into the MP unit, where it is equivalent to that unit's S_d foliation (Fig. 4, A–A′). F_2 fold hinges and $L_{1\times2}$ intersection lineations plunge approximately down the dip of S_2 (Fig. 7c). In some exposures, mesoscopic F_2 folds are demonstrably sheath-shaped. Quartz veins on the limbs of some F_2 folds have been rodded and pulled-apart into boudins, the long axes of which plunge down-dip. These boudins have themselves been pulled-apart into stubbier fragments and extended subparallel to a strong down-dip stretching lineation, L_{2e} (Fig. 7d). L_{2e} is defined by ribbon-shaped quartz grains, elongate micaceous bundles, and fibers of quartz, chlorite, white mica or tremolite that link microboudinaged fragments of albite or clinozoisite.

In pelitic rocks, M_1 minerals and the S_1 foliation are commonly preserved in microlithons of the S_2 foliation. These include quartz, chlorite, white mica, albite, and rarer chloritoid and garnet. Chlorite pseudomorphs after garnet are common, indicating that garnet was probably a widespread mineral in the northern half of the map area prior to M_2 retrogression. These are variably flattened in the S_2 foliation, and are in some cases decorated by coronas of fresh biotite (Fig. 5d). In addition to garnet and chloritoid, lath-shaped aggregates of chlorite+albite+quartz with amphibole cross-sections may be pseudomorphs of M_1 glaucophane such as those reported by Gottschalk (1990) farther east. Rarer pseudomorphs with square cross-sections, now consisting of chlorite+white mica+quartz±clinozoisite, or quartz+calcite+albite+clinozoisite+white mica, may have been lawsonite (Fig. 6a). Chloritoid typically occurs as large (millimeters to 1 cm), graphite- and inclusion-rich porphyroblasts that are kinked by D_2 crenulations (Fig. 6b).

M_2 is a pervasive greenschist facies overprint that was syntectonic with development of the S_2 foliation, the dominant structural fabric in the Schist Belt. In pelitic schists, S_2 is a differentiated crenulation cleavage defined by anastomosing cleavage seams rich in graphite and mica that alternate with microlithons rich in quartz and albite. Rocks with mafic and intermediate composition are massive to schistose and contain an M_2 assemblage of actinolite, albite, epidote–clinozoisite, chlorite, sphene ± white mica ± quartz. In pelitic rocks, minerals that are syntectonic with respect to S_2 include albite, quartz, white mica, chlorite ± clinozoisite or zoisite ± calcite ± tremolite, and possibly chloritoid. Biotite is rare, and its occurrence is probably compositionally controlled. These assemblages indicate metamorphism under greenschist facies conditions, possibly transitional into epidote–amphibolite facies conditions. M_2 micaceous minerals occur as fibrous beards or neoblastic flakes aligned along the S_2 foliation, although locally they occur as decussate aggregates that appear to be late- or even post-kinematic.

Albite porphyroblasts with D_2 pressure fringes of inclusion-free albite or fibrous quartz are abundant in the schists. These porphyroblasts are clearly syntectonic with D_2, as they overgrow variably straight, sigmoidal, or F_2-crenulated internal inclusion trails and have margins that are variably truncated or anastomosed by S_2 cleavage films (e.g. Bell *et al.* 1986). Defined by opaques and mica, the inclusion trails are parallel to S_1 where that foliation is preserved in microlithons of the D_2-crenulated matrix. The trails deflect into parallelism with the S_2 foliation of the matrix along the edges of the porphyroblasts, but are at high angles to S_2 in the centre of porphyroblasts. The trace of S_1 preserved in these porphyroblasts commonly dips more steeply to the south than the external matrix foliation, S_2 (Fig. 6c). Assuming minor rotation of the porphyroblast, this relationship suggests that S_1 originally dipped more steeply than S_2. Although we cannot discount the possibility of porphyroblast rotation, oriented thin sections across the

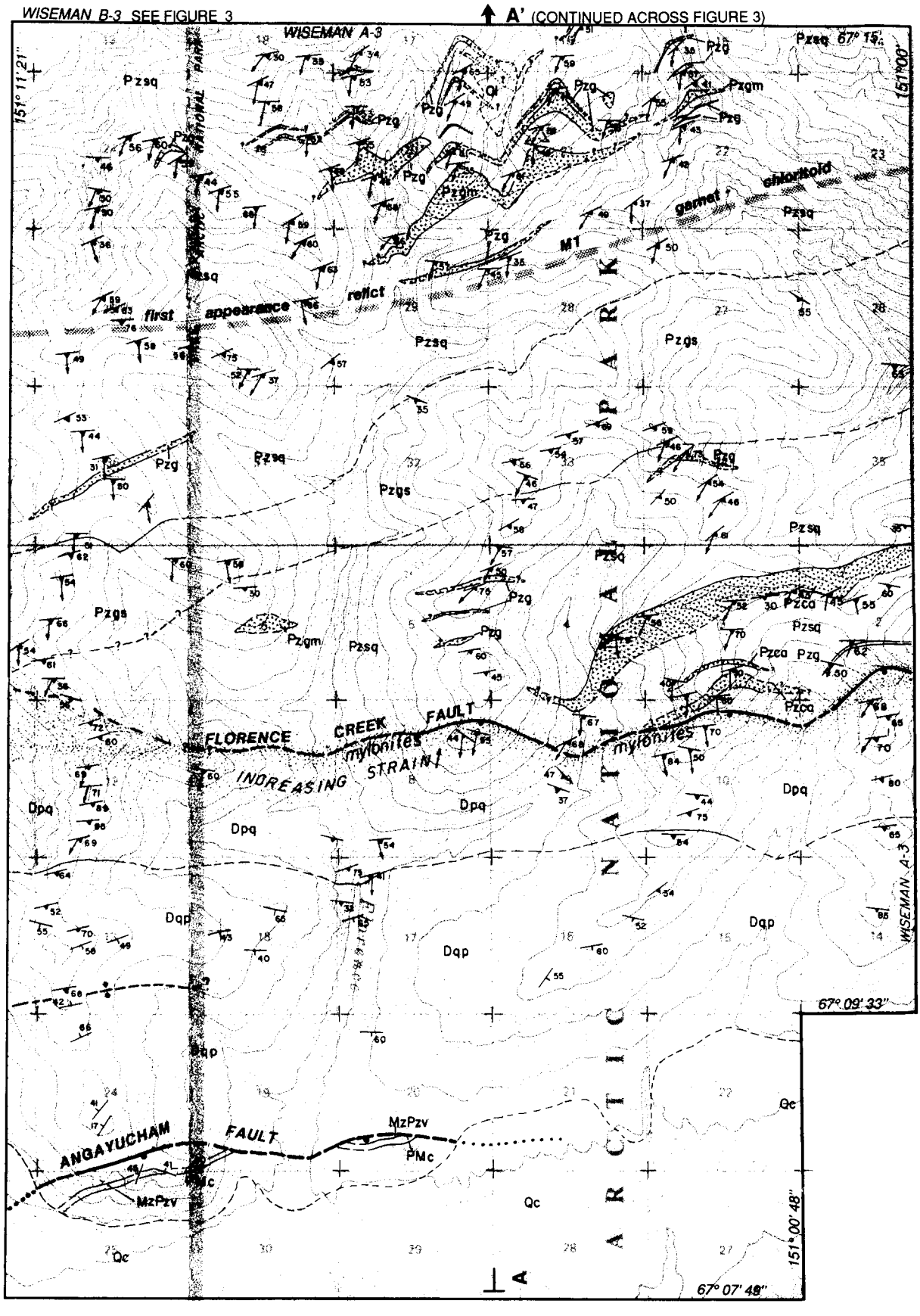

Fig. 2. Simplified geologic map of the southern part of the study area in the south-central Brooks Range.

region reveal variable inclusion trail geometries that reflect overgrowth of the porphyroblasts across pre-existing F_2 crenulations. Thus, the internal and external foliations do not represent the same foliation but formed at a high angle to one another. For this reason we believe that the albite porphyroblasts cannot be used as D_2 sense of shear indicators.

The most intensely deformed rocks, showing the least

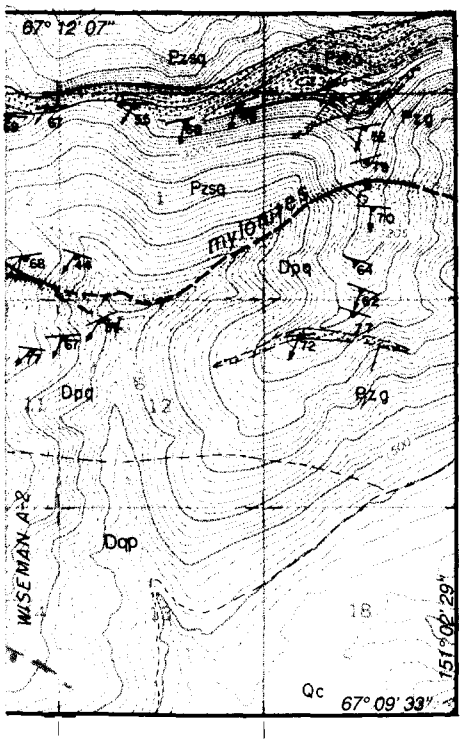

LEGEND

Ql — Quaternary landslide deposits

Qc — Quaternary cover

Angayucham Terrane
(Devonian to Jurassic)

MzPzv — Altered amygdaloidal pillow basalt

PMc — Radiolarian chert and argillite (Late Mississippian -Early Pennsylvanian)

Phyllite-Metagreywacke unit
(Devonian ?)

Dqp — Quartzose metasandstone with lesser slate and phyllite. Relict bedding and detrital textures

Dpq — Phyllite with lesser quartz-rich metasandstone

MP unit

Southern Brooks Range Schist Belt
(Precambrian? to Devonian)

Pzsq — Graphitic quartz mica schist (chlorite+white mica+ albite+quartz) and minor quartzite with lenticular greenstone bodies and rare marble, calc-schist and calc-silicate

Pzgs — Black graphitic quartz mica schist (chlorite+white mica+albite+quartz)

Pzca — Schistose meta-andesite (white mica+quartz+zoisite/ clinozoisite+epidote+actinolite+albite+chlorite)

Pzg — Schistose greenstone (sphene+ zoisite/ clinozoisite+epidote+albite+actinolite+chlorite)

Pzgm — Massive mafic greenstone (greater % actinolite than Pzg)

QMS unit

Pzmcs — Pzcs: Micaceous albite calc-schist, locally graphitic(clinozoicite/epidote+albite+ white mica+ chlorite+quartz+calcite)

Pzm: Schistose to massive white to light grey marble

Micaceous albite calc-schist interlayered with white marble units

Pzcb — Micaceous albite calc-schist interlayered with black marble units

CS unit

STRUCTURAL SYMBOLS

Contact, dashed where inferred or approximately located, dotted where concealed, queried where speculative

Strike and dip of bedding

Strike and dip of foliation (S_2) and trend of mineral elongation or stretching lineation

Normal-separation fault, ball on downthrown side. Dashed where inferred or approximately located, dotted where concealed, queried where speculative.

Overturned D_2 antiform, synform, showing direction of plunge

SCALE

0 1 2 3 4 km

Fig. 2 (*continued*).

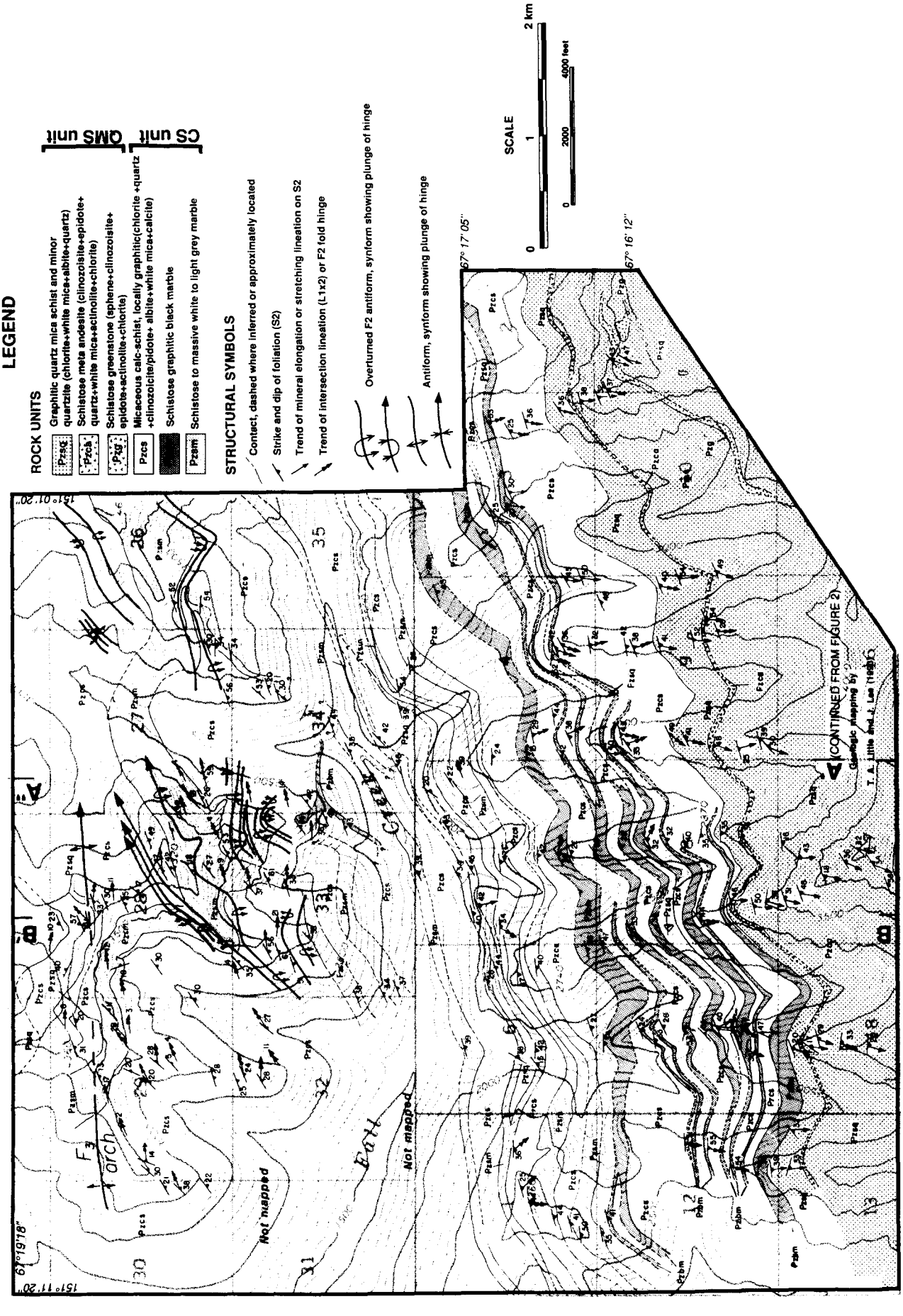

Fig. 3. Geologic map of the northern part of the study area, near Fall Creek, covering the area shown as Wiseman B-3 Quadrangle on Fig. 2.

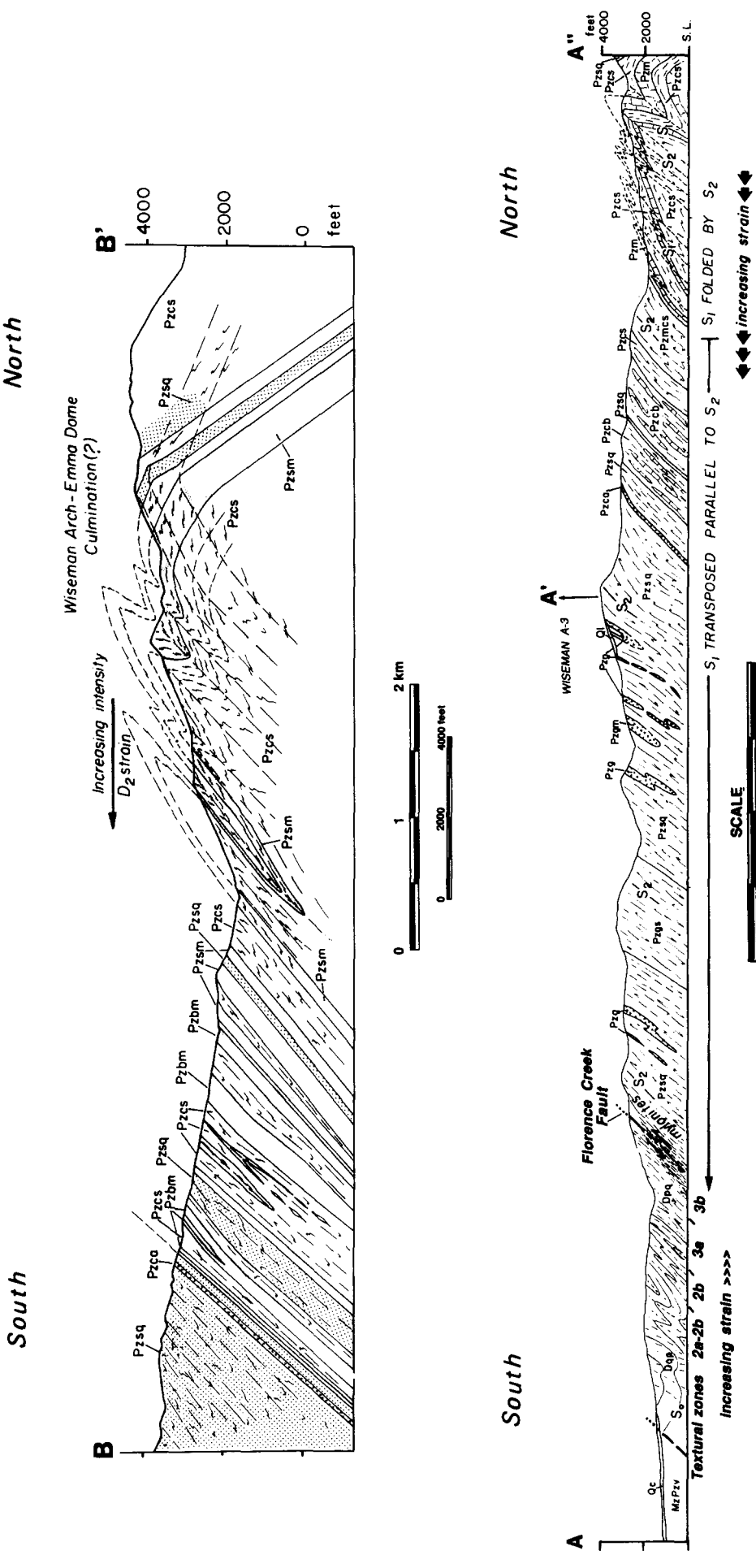

Fig. 4. Geologic cross-sections. No vertical exaggeration. (a) Section A–A'. See Figs. 2 and 3 for location. Note that this section extends from Fig. 2 into the area of Fig. 3. (b) Section B–B'. See Fig. 3 for location.

evidence for recovery processes, occur within 300 m of the FCF. Here, quartz grains in mylonitic schists have been dynamically recrystallized into fine-grained aggregates, have a strong lattice preferred orientation, and commonly define a grain shape fabric which is oblique to S_2 (fig. 4 in Law *et al.* 1994). These flaggy quartzitic rocks are Type II *S–C* mylonites (Lister & Snoke 1984) and contain late-stage top-to-the-south extensional shear bands that post-date S_2.

Farther north quartzitic rocks remain strongly lineated *L–S* tectonites, but are slightly coarser grained. Quartz is largely recrystallized and granoblastic in thin section (e.g. Fig. 6c). This observation suggests that the rate of diffusion-controlled recovery in quartz during D_2 was greater than the rate of work-hardening associated with dislocation glide in that mineral. There does not appear to be a significant change in M_2 grade across the study area; however, it is clear that new growth and the grain size of M_2 minerals and the degree of annealing and recrystallization in quartz generally increase northwards.

In the QMS unit, microstructures in quartzose layers indicate a predominance of top-down-to-the-south (extensional) sense of shear (Fig. 7). Nineteen samples that contain oblique quartz grain-shape fabrics indicative of top-down-to-the-south shear also have preferred quartz *c*-axis patterns with strongly asymmetric crossed- or single-girdle patterns indicative of the same shear sense (Law *et al.* 1994). In addition, these samples also contain other kinematically diagnostic microstructures, such as asymmetric mica fish in Type II *S–C* mylonites and albite porphyroclasts with sigma-type asymmetric recrystallized tails (Passchier & Simpson 1986). An additional six samples that lack an obvious quartz grain-shape fabric have well defined top-down-to-the-south asymmetric *c*-axis patterns (figs. 8 and 10 in Law *et al.* 1994). Two samples in the central part of the QMS unit have *c*-axis fabrics and oblique grain-shape alignments consistent with a top-up-to-the-north component of shear. North of these two samples, four oblique quartz grain-shape fabrics, five *c*-axis fabric diagrams and 10 extensional shear band observations all indicate a top-down-to-the-south sense of shear. We believe that the two samples exhibiting opposite senses of shear may represent zones of conjugate shear or flow within the broader zone of deformation affected by D_2 rather than relict D_1 fabrics. Late-stage extensional shear bands spaced 5–20 cm apart are sparsely distributed throughout the QMS unit. They dip more steeply south than S_2 (Fig. 7e) and indicate top-down-to-the-south movement (see also Gottschalk 1990) (Fig. 7). Despite the above-cited evidence for a prevailing top-down-to-the-south shear sense, many specimens of these *L–S* tectonites lack shear-diagnostic microstructures and have symmetric pressure shadows compatible with coaxial deformation involving bulk shortening perpendicular to foliation and extension parallel to lineation (see also quartz petrofabric data of Law *et al.* 1994, fig. 6).

Calc-schist-rich unit of the Schist Belt (CS)

Micaceous calc-schist, pure and graphitic marble and minor pelitic schist of the CS unit structurally underlie the QMS unit along a contact that is overprinted by, and subparallel to, S_2 (Figs. 3 and 4, B–B′). These rocks contain the same structural elements as overlying rocks of the QMS unit; however, the intensity of D_2 strain affecting the CS unit decreases northwards.

South of Fall Creek, the CS unit is structurally similar to the QMS unit. At least two markers of pelitic and quartzitic schist occur interbedded within the otherwise calcareous CS sequence (Pzsq unit, Fig. 3). Structural fabrics in these quartzose markers are identical to those found in lower parts of the QMS unit. The thickly interbedded sequence is deformed into multiple orders of F_2 folds, ranging from microscopic crenulations of the bedding-parallel S_1 foliation to folds with half-wavelengths of over 1 m. S_2 is axial planar to these tight or isoclinal folds and dips moderately to the south (Figs. 4, B–B′, and 7d). $L_{1\times2}$ intersection lineations (Fig. 7c) form a girdle about a cluster of down-dip L_{2e} stretching lineations (Fig. 7d). D_2 strains are especially high in black marble units (Pzbm), where S_2 is a thinly fissile schistosity, and the down-dip L_{2e} lineation is defined by strongly elongate coarse calcite crystals that overgrow S_2-parallel inclusion trails of graphite.

M_2 minerals that grew or recrystallized syntectonically with D_2 include quartz, calcite, white mica, albite, chlorite ± clinozoisite–epidote. Quartz, although chiefly granoblastic, locally has undulatory extinction. Albite porphyroblasts have the same helicitic textures and inclusion-free pressure fringes as those described for rocks in the QMS unit. White mica occurs in fibrous pressure fringes adjacent to albite porphyroblasts, as recrystallized grains in the hinges of some crenulation microfolds, and locally as aligned neoblasts growing in S_2 cleavage seams. In some rocks, white micas are present in post-kinematic sprays. Chlorite is present in pressure fringes, as local dilation-site fillings in the hinges of F_2 crenulations, and as idioblastic or flattened

Fig. 5. Photographs of the metagraywacke–phyllite unit and Schist Belt. (a) Weakly-deformed textural zone 2a metasandstone in metagraywacke subunit of MP unit, showing contact (S_0) between psammitic and pelitic beds. Note that foliation here cuts original bedding at a moderate angle and anastomoses around relict detrital grains. Width of photograph is 3.6 mm. Plane light. (b) Strongly deformed textural zone 3a metasandstone in phyllite subunit of MP unit, showing spindle-shaped relict detrital quartz grains, fibrous mica–quartz beards on sides of grains, and dark, opaque-rich pressure solution seams parallel to S_d. Quartz-rich seams and veins in these rocks have strong preferred *c*-axis patterns. This sample is structurally lower than that of (a) and is cut perpendicular to foliation and parallel to elongation lineation L_{de}. Width of photograph 1.44 mm. Plane light. (c) Top-to-the-south extensional shear band in phyllite subunit of MP unit. Note pocket knife for scale. (d) Retrogressed M_1 garnet in QMS unit. Dominant cleavage is S_2 (left-to-right). Small, variably flattened garnets with retrograde rims of M_2 chlorite and lesser M_2 biotite (dark material on edge of pseudomorph—see arrows). Quartz, white mica and albite are additional constituents. Sample is cut perpendicular to S_2 foliation and parallel to elongation lineation L_{2e}. Width of photograph 3.6 mm. Plane light.

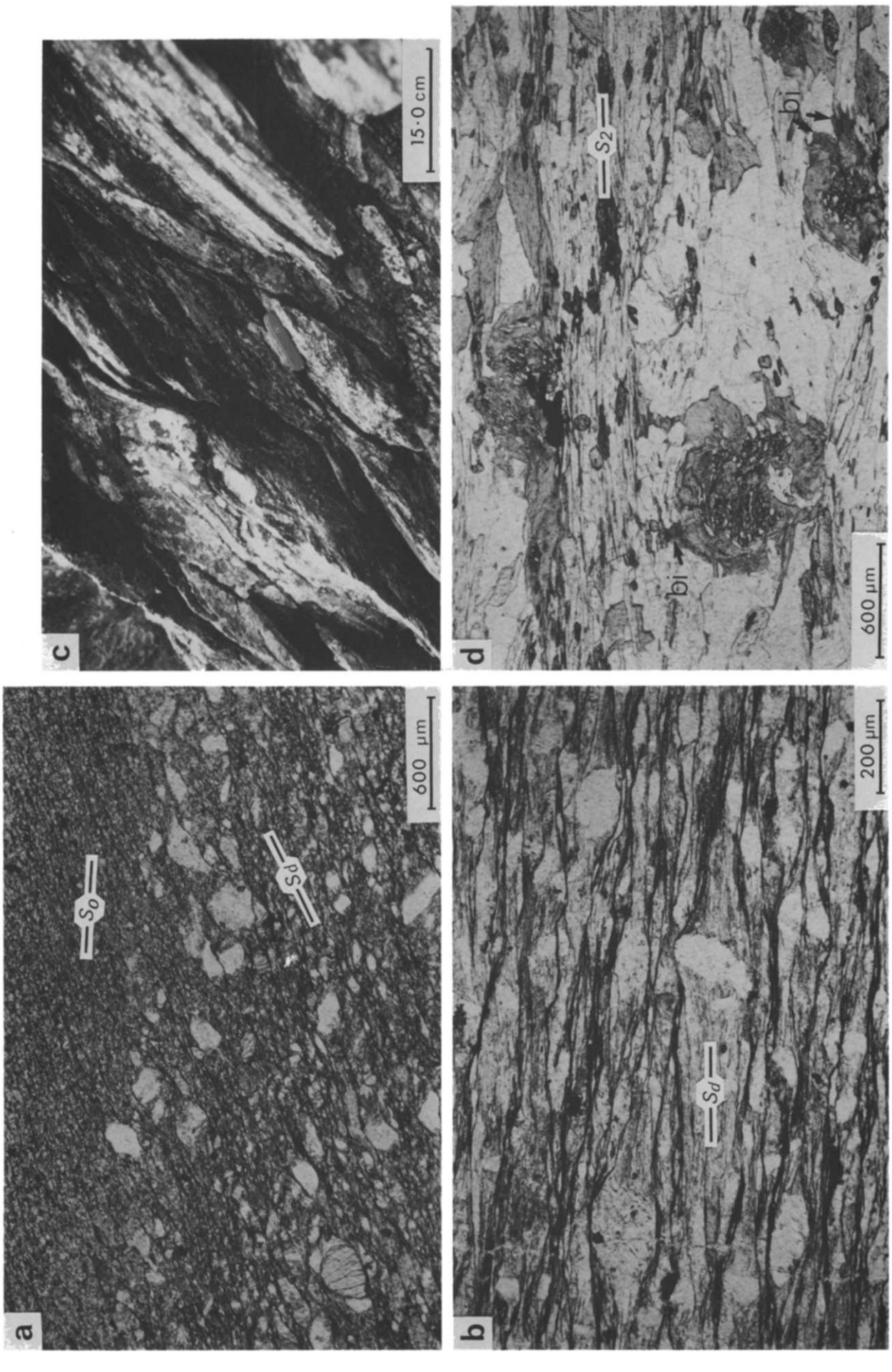

Fig. 5.

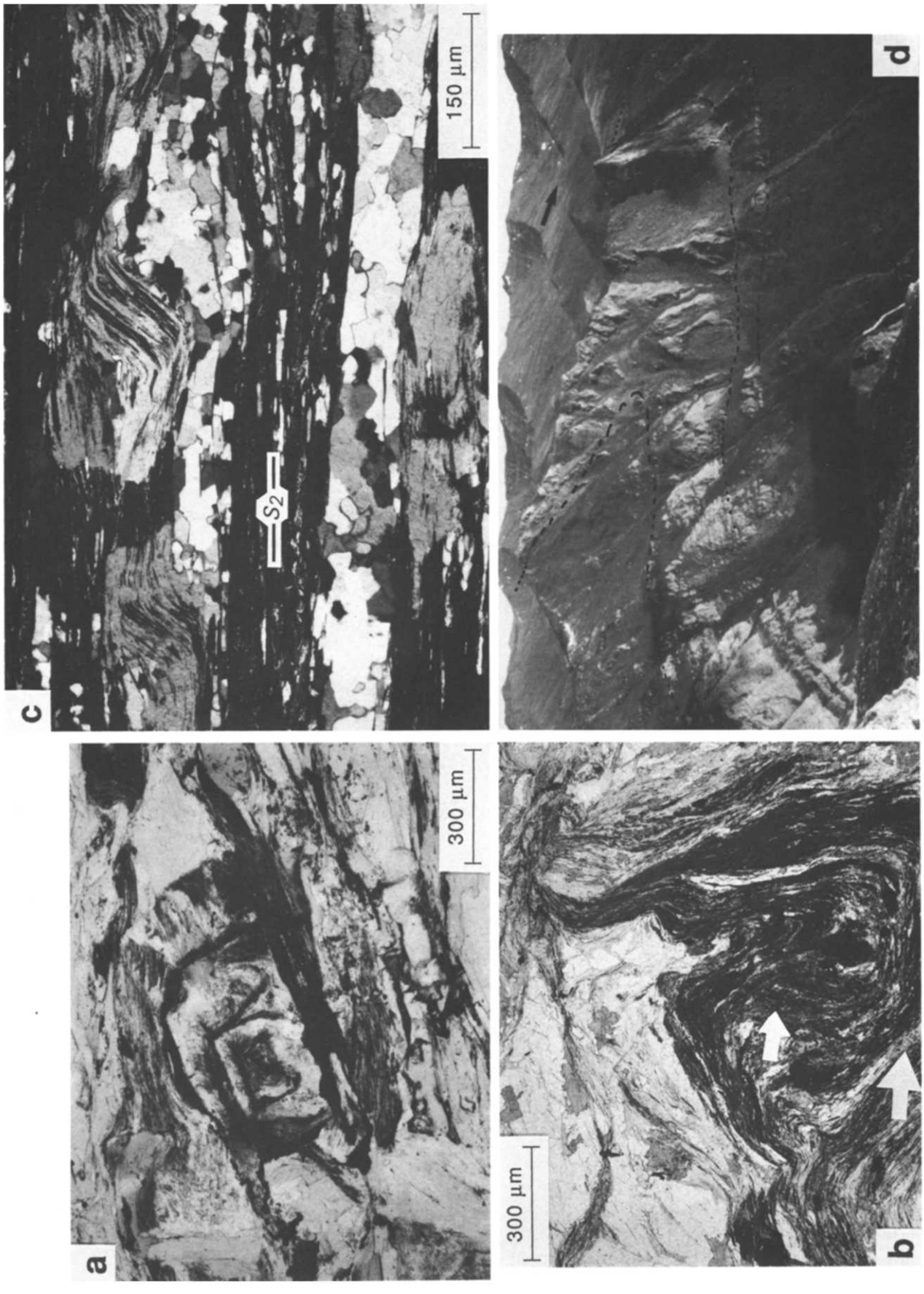

Fig. 6.

pseudomorphs after M_1 garnet. Few microstructures diagnostic of shear sense were observed in the CS unit (Fig. 7).

In the region northwards from Fall Creek, S_2 maintains its moderate southward dip, but the intensity of D_2 strain decreases. Compared to its expression in identical rock types farther south, S_2 is more widely spaced and microlithon boundaries are gradational. In these apparently less strained rocks, the down-dip stretching lineation, L_{2e}, is only rarely detectable (Fig. 7h). Lower strains are also reflected in part by decreased appression of F_2 folds, which north of Fall Creek have interlimb angles of 40–50° rather than being tight to isoclinal. There, one can routinely measure the discordant attitudes of local S_1 (Fig. 7g) and S_2 (Fig. 7h), and map the axial surfaces of large F_2 folds deforming marble units (Figs. 3 and 4, B–B′). Unlike F_2 sheath-folds farther south, these folds are nearly cylindrical. In the vicinity of Fall Creek and farther north, the mean trend of $L_{1\times2}$ lineations and F_2 fold hinges swings to a more easterly azimuth (Figs. 7g & h). We interpret the southward shift in mean lineation trend towards the down-dip stretching direction, L_{2e}, to reflect a strain-related rotation away from an original lineation trend that was more E–W (e.g. Sanderson 1973). Using mean values for $L_{1\times2}$ on either side of Fall Creek, the observed ~60–70° change in pitch of the lineations towards parallelism with L_{2e} is consistent with an XY strain ratio of at least 30. For further constraints on the magnitude of D_2 strain that are based on quartz petrofabric data, see the companion paper by Law *et al.* (1994).

North of Fall Creek the S_1 foliation is not entirely transposed and M_1 minerals syntectonic with that fabric are better preserved. Idioblastic porphyroblasts of M_1 garnet and chloritoid growing in the S_1 foliation are both common. In addition, some calc-schists contain coarse poikiloblasts of brown calcite with inclusions of clinozoisite and white mica that are possibly pseudomorphs after M_1 lawsonite. M_2 minerals in this area reflect the same metamorphic grade as in rocks farther south.

F_2 folds deforming thick marble units (Pzsm) and their enclosing calc-schists (Pzcs) are spectacularly exposed north of Fall Creek (Figs. 3 and 6d). The asymmetric folds have short limbs that dip more steeply south than their long limbs, and contain cascades of parasitic folds. S_2 is arrayed into a convergent cleavage fan, a geometry that is partly responsible for the girdled distribution of poles to mesoscopic F_2 axial planes plotted on Fig. 7(h). The other reason for this girdled pattern is the local occurrence of late- to post-metamorphic folds of S_2.

Late- to post-metamorphic structures in the Schist Belt

Folds deforming the dominant S_2 fabric are uncommon. South of Fall Creek, S_2 is locally deformed by F_3 folds with half-wavelengths of a few tens of centimetres to several meters. The cores of these close folds have a spaced, gradational crenulation cleavage, S_3, that dips to the south subparallel to the regional mean attitude of S_2. S_3 intersects S_2 to form an E-trending $L_{2\times3}$ lineation (Fig. 7f). F_3 folds are restricted to thick, tabular units of graphitic marble (Pzbm) and do not affect adjacent calc-schist units (Pzcs). Although no sense of F_3 fold asymmetry was observed, these intrafolial folds may have resulted from concentration of simple shear deformation into weaker carbonate units during later phases of a progressive D_2 deformation event. According to this strain-partitioning interpretation, local perturbations in the velocity field within the tabular carbonate layers may have led to folding of the foliation (e.g. Platt 1983, Ghosh & Sengupta 1987).

Along the northern edge of the study area, S_2 is warped from a gentle southerly dip to a gentle northerly dip to define a broad foliation arch (Fig. 3). Mean S_1 steepens across this post-metamorphic fold to become subvertical (Fig. 4, B–B′).

INTERPRETATION

Regional correlation of metamorphic fabrics

A penetrative S-dipping crenulation cleavage developed during lower to upper greenschist-facies metamorphism is the dominant structural element of the Brooks Range Schist Belt and has been described in some detail by various workers for hundreds of km along strike within the range (Gilbert *et al.* 1977, Dillon *et al.* 1981, Hitzman 1984, Christiansen 1989, Gottschalk 1990). Other recent work suggests that the same (?) fabric may extend beyond the Schist Belt to overprint rocks as far north as the Endicott Mountains allochthon and Doonerak window (e.g. Handschy 1988). In the Schist Belt, metamorphic rocks that exhibit this foliation form a conspicuous belt of furrowed ridges that compose the southern foothills of the Brooks Range (Fig. 6d). This foliation also defines a series of broad arches or folds such as the Cosmos Hills and Kalaruvik Arch to the north, Emma dome and the Wiseman arch (Figs. 1 and 9b). This regional foliation represents large strains in that it tightly crenulates or transposes an older foliation,

Fig. 6. Photographs of Schist Belt, continued. (a) Possible pseudomorph after lawsonite consisting of white mica, quartz and lesser chlorite. Note square outline and strongly curved inclusion trails. Width of photograph is 1.5 mm. Plane light. (b) Large graphite- and inclusion-ridden chloritoid porphyroblast. Arrow points to remaining patches of mineral. Note that inclusion trails (S_1) and the porphyroblast itself are both strongly kinked about S_2. Width of photograph is 1.5 mm. Plane light. (c) Non-mylonitic quartz–mica schist of Pzqms unit showing syntectonic albite porphyroblasts overgrowing sigmoidal crenulations of an internal foliation (S_1), defined by graphitic inclusion trails. In this sample S_1 dips more steeply to the south (left) than S_2 (left-to-right foliation). Sample is cut perpendicular to foliation and parallel to elongation lineation L_{2e}. South is on the left. Crossed polars. (d) Photograph looking southeast of ridges in the Schist Belt defined by the S-dipping S_2 foliation in background (black arrow along trace of foliation with topography). Gently inclined, map-scale folds of thick marble units in foreground (highlighted) have S_2 axial plane foliation.

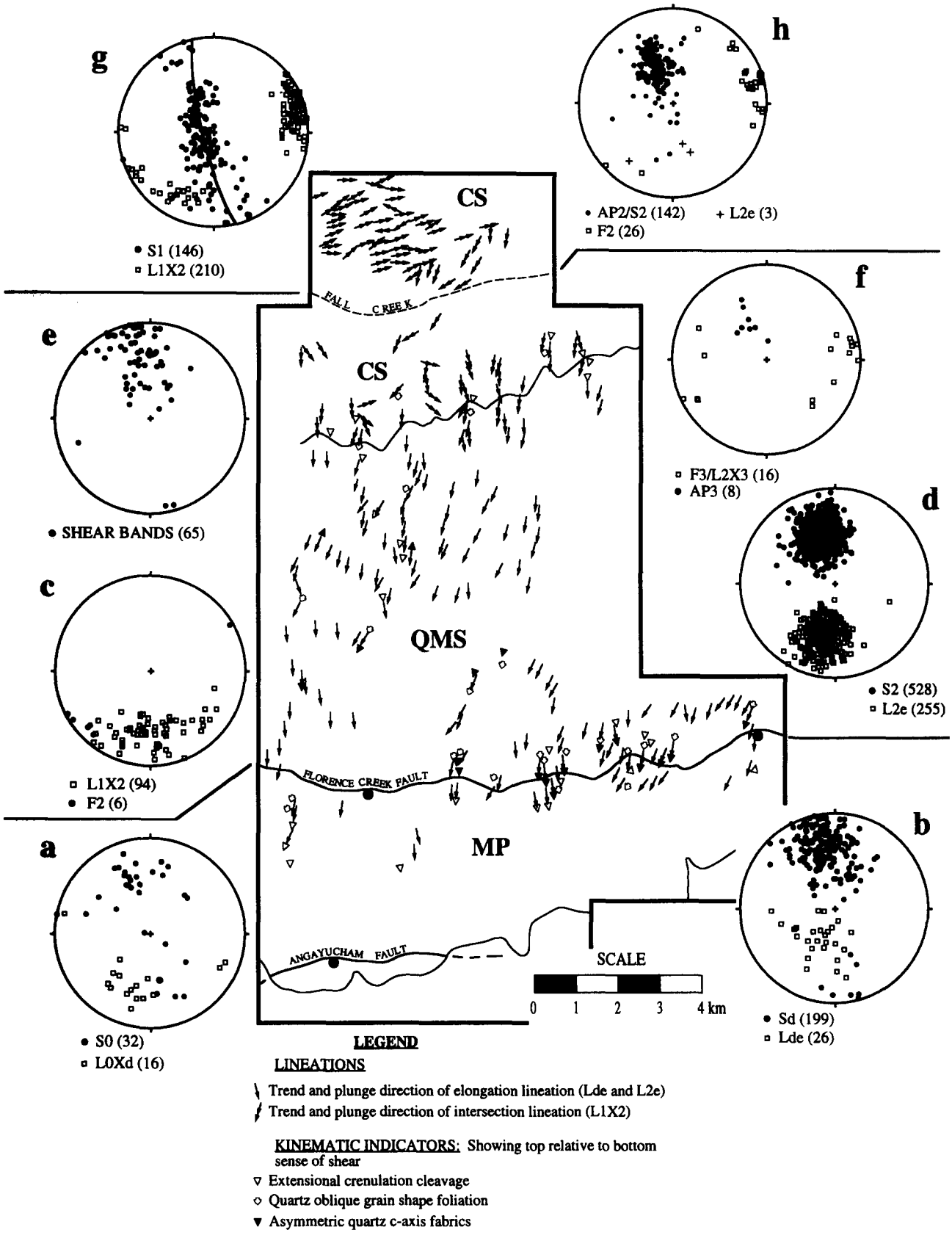

Fig. 7. Simplified geologic map of the study are showing intersection and elongation lineations and the location of structural domains. Structural data plotted on lower-hemisphere, equal-area projections (number of measurements given in parentheses). In the MP unit: (a) poles to S_0 (solid circles) and $L_{0\times d}$ intersection lineation (open squares); and (b) poles to S_d (solid circles) and L_{de} elongation lineation (open squares). In the quartz–mica schist (QMS) and calc-schist (CS) units south of Fall Creek: (c) $L_{1\times 2}$ (open squares) and F_2 fold axes (solid circles); (d) poles to S_2 (solid circles) and L_{2e} elongation lineation (open squares); (e) poles to shear bands (solid circles); and (f) poles to F_3 axial planes (solid circles) and F_3 fold axes and $L_{2\times 3}$ intersection lineations (open squares). In the calc-schist (CS) belt north of Fall Creek: (g) poles to S_1 (solid circles) and $L_{1\times 2}$ intersection lineation (open squares); and (h) poles to F_2 axial planes and S_2 (solid circles), F_2 fold axes (open squares) and L_{2e} elongation lineation (crosses).

is locally represented by mylonitic fabrics, contains a consistently oriented and well-developed down-dip mineral elongation lineation, and is locally axial planar to sheath folds. Large-magnitude strains (XY strain ratio of >30) are also indicated by an apparent ~70° rotation of $L_{1\times2}$ intersection lineations from gentle plunges to nearly down-dip trends as one moves north to south in our particular study area. The S_2 foliation described here is probably equivalent to the S_{1b} crenulation foliation described along the Trans-Alaska Pipeline route by Gottschalk (1990), and to the dominant foliation described to the west of our study area by Dillon *et al.* (1981). Gottschalk (1990), however, did not describe a stretching lineation or mylonitic textures in correlative quartz–mica schists along the Pipeline route, thus the intensity of D_2 strain may be less there. Many of the differences between our observations and those of Gottschalk (1990) are possibly related to more intense development of the S_2-related L–S tectonite fabric near Florence Creek. The Wiseman arch of Gottschalk (1990) and its western continuation, the Emma dome (Dillon *et al.* 1989), occur in a structurally analogous position to the foliation arch in S_2 described at the northern part of the map area, and these may be equivalent antiforms.

Our interpretation that the S_2 foliation developed during transposition and greenschist-facies overprinting of an older, blueschist-facies foliation accords well with the work of Gottschalk (1990). These high-P–low-T assemblages probably formed at deep structural levels of the Brooks Range fold and thrust belt during crustal thickening and southward continental underthrusting in Jurassic–Early Cretaceous time (Armstrong *et al.* 1986, Gottschalk 1990). In the study area, the only remaining evidence for high-p/low-t metamorphism are remnants of an early foliation (our S_1), and a poorly preserved and retrogressed M_1 assemblage that includes garnet and chloritoid, and pseudomorphs that may have been glaucophane and lawsonite. Inclusion trains of S_1 in albite porphyroblasts, if unrotated, suggest that S_1 dipped more steeply than S_2.

Extensional kinematic interpretation of D_2 *event*

Our conclusions differ from those of other workers in the Schist Belt primarily in our kinematic interpretation of S_2, the pervasive S-dipping foliation that is the dominant metamorphic fabric in the southern part of the Brooks Range orogen. Whereas Gottschalk (1990) also recognised top-down-to-the-south extensional shear bands in the Schist Belt, he argued that the high-strain S_2 fabric (his S_{1b}) pre-dating these shear bands is unrelated to crustal extension. Our new microstructural observations together with the quartz petrofabric data of Law *et al.* (1994), which were collected from high-strain L–S tectonites formed during D_2, suggest that this regionally widespread, penetrative foliation formed during deformation with a top-down-to-the-south shear. We attribute this syn-D_2 sense of shear to crustal extension because: (1) it is associated with and formed as a consequence of development of the regionally S-dipping high-strain foliation; (2) because it is sympathetic with the sense of dip-separation on the pre- to syn-D_2, Florence Creek normal fault (see below); and (3) because it is sympathetic with the sense of movement on post-S_2 extensional shear bands. D_2 strain increases in intensity towards the S-dipping FCF, suggesting that the D_2 strain was intensified along this contact and that this zone represents a shear zone with top-down-to-the-south displacement.

If one considers the alternative that the S_2 was thrust-related then the hangingwall of the observed shear zone would represent the sole of a thrust nappe and should consist of higher-grade metamorphic rocks. The hangingwall of the FCF, however, consists of very-low-grade rocks (MP unit) representing a higher structural level of exposure than the underlying schists. The FCC, therefore, has a normal sense of dip-slip separation. Most of the MP unit contains a slaty or rough cleavage formed chiefly by pressure solution under very low-grade conditions. The appearance of metamorphic biotite and crystal-plastic deformation textures in quartz indicates that temperatures probably increased in the hangingwall towards the FCF, where the foliation locally becomes phyllitic. In contrast, schists in the structurally underlying QMS unit are completely recrystallized, polydeformed schists that locally retain evidence for a early high-P–low-T event. We infer that these two packages of rocks, metamorphosed at different crustal levels during the M_1 event, were juxtaposed prior to (or during) development of the S_d–S_2 foliation. We emphasize that this foliation overprints rocks on both sides of the FCF. In contrast to the conclusions of Gottschalk & Oldow (1988), our observations suggest the hangingwall of the FCF largely escaped the ductile strain that imprinted S_1 on the more complexly deformed footwall, as there is only very localized evidence in the MP unit for a pre-S_d foliation, and no obvious evidence for early high-P–low-T metamorphism.

It is interesting that mylonitic fabrics and evidence for crystal-plastic deformation are present in both the hangingwall and footwall of the Florence Creek fault zone (S_d in the MP unit; S_2 in the Schist Belt). This S-dipping fabric contains a down-dip stretching lineation and preserves microstructures indicative of top-down-to-the-south shear (Law *et al.* 1994). Both units also contain late-stage, down-to-the-south ductile shear bands. In the Cosmos Hills (Figs. 1 and 9b), Box (1987) and Christiansen (1989) described similar extensional faults of post-Early Cretaceous age where a strong foliation overprints inferred fault contacts between Schist Belt rocks, the MP unit and the Angayucham Terrane. The foliation is also present as a weak fabric in overlying fault-bounded Cretaceous sediments of the Yukon–Koyukuk basin. Thus, if contacts between units along the southern flank of the range are normal faults, ductile deformation of inferred extensional origin is synchronous with and/or post-dates motion on these faults.

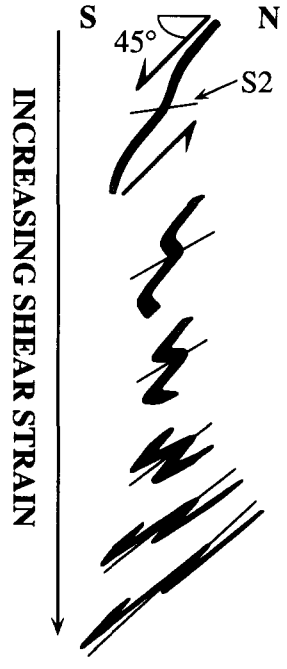

Fig. 8. Schematic diagram illustrating formation of N-vergent asymmetric folds as a result of top down-to-the-south sense of shear (normal sense simple shear) (after Ramsay *et al.* 1983). Original steeply S-dipping attitude of S_1 is suggested by trace of that foliation as preserved in albite porphyroblasts in the QMS unit.

N-vergent asymmetric folds in the Brooks Range Schist Belt such as those described north of Fall Creek in the present study have been cited as evidence of pervasive top-to-the-north tectonic transport related to the Brookian orogeny (Till *et al.* 1988, Gottschalk 1990, Patrick *et al.* 1991, Till *et al.* 1993). However, fold asymmetry is strongly dependent on the original mean orientation of the folded surface (generally unknown), and need not arise from any prevailing bulk sense of shear (Ramsay & Huber 1983, p. 28, Williams & Price 1990). Thus, in view of our evidence for a top-down-to-the-south sense of shear (Law *et al.* 1994), we view the N-vergent asymmetry of map-scale F_2 folds observed at structurally deep levels of the CS unit as reflecting the obliquity between the original mean attitude of S_1 and the orientation of the younger S_2 foliation. For simplicity, the model in Fig. 8 depicts a case of progressive simple shear, and implies that mean S_1 dipped steeply to the south prior to S_2 development. If one assumes only minor porphyroblast rotation (e.g. Bell & Johnson 1989), the latter relationship is consistent with the angular relation observed between S_1 preserved in albite prophyroblasts and matrix S_2 in the QMS unit. Numerous other strain paths, with or without a component of normal-sense simple shear, could similarly result in folds that have a N-vergent sense of asymmetry. Thus fold asymmetry is an unreliable sense-of-shear indicator.

Figure 9 contrasts simplified structural cross-sections of the southern Brooks Range (Figs. 9b & c) with a relatively well-constrained crustal cross-section through an extensional metamorphic core complex in the Basin and Range province (Snake Range) (Fig. 9a). The nature and extent of extension-related ductile strain is also very generally and schematically portrayed in these examples. We do this in order to illustrate some of the similarities as well as important differences in the scale and geometry of extensional structures developed in the two different regions, both of which were involved in a prior history of crustal thickening.

The similarities include: (1) increasing development of mylonitic fabrics structurally upward and towards overlying normal fault systems; (2) increasing evidence for coaxial deformation with structural depth and away from bounding faults; and (3) decreasing intensity of extension-related fabrics in the direction away from bounding normal faults, with increased preservation of older fabrics in this direction. In the case of the Brooks Range, these older fabrics are convergent-related blueschist grade fabrics and metamorphic assemblages.

Important differences include, first, that mylonites in quartzose rocks are less well developed in the Brooks Range. Temperature-controlled recovery processes in quartz outpaced the rate of work-hardening associated with dislocation glide in that mineral at most levels of exposure except for the top of the Schist Belt and in the base of the MP unit in our map area. Thus true mylonitic rocks are restricted to the FCF zone. If this fault system is analogous to those in the Basin and Range, it must be a more deeply exhumed portion of such a structure or represent lesser total strains. Alternatively, the ductile fabric in question might actually overprint a normal fault which moved earlier under brittle conditions. One could argue that this is more clearly the case in the Cosmos Hills, where high-strain, top-to-the-south ductile fabrics overprint the faults that bound both the Angayucham terrane and the base of the Cretaceous clastic section (e.g. Christiansen 1989). This possible overprinting of brittle structures by ductile fabrics is not generally characteristic of the present levels of exposure of extensional fault systems in the Basin and Range, although it may be the case at deeper levels of exposure or in regions where syn-extensional magmatism has led to increased temperatures in the upper crust. Third, normal fault systems in the Basin and Range still preserve planar geometries while the fault systems developed along the southern flank of the Brooks Range appear to have been folded in latest Cretaceous or Tertiary time. This is evident from: (1) open to tight folds that affect the Cretaceous clastic section in the central Yukon–Koyukuk basin (Cushing & Gardner 1989); (2) folding of the basal unconformity of the Cretaceous section as shown in the cross-sections of Dillon *et al.* (1981, 1987); and (3) by regional folds of the Schist Belt, such as the Cosmos arch (Fig. 9), which have led to the ultimate exhumation of these metamorphic tectonites in the Early Cenozoic, as deduced from apatite fission-track data (Murphy *et al.* 1991). If the comparison with extensional structures in the Basin and Range is valid, these differences may indicate increasing temperatures during the later stages of extension in the southern Brooks Range and adjacent Yukon–Koyukuk basin, prior to cooling of the rocks below the Ar closure temperatures for white mica and biotite (see below).

Tectonic context and timing of extensional deformation

Gottschalk & Oldow (1988) argued that normal faulting along the southern flank of the Brooks Range Schist Belt accommodated localized gravitational collapse of the upper crust above a zone of deeper-seated out-of-sequence thrusting and crustal thickening (after Platt 1986). According to their model, this localized extensional deformation occurred during a mid-Cretaceous phase of the Brookian orogeny. They attribute the pervasive greenschist-facies ductile fabric in the Schist Belt to emplacement of deep-seated thrust nappes. In an alternative view, Miller & Hudson (1991, 1993) argued that mid-Cretaceous extension in northern Alaska involved the entire crust and resulted in the formation of marine turbidite basins across the tectonically thinned hinterland of the fold–thrust belt (Miller & Hudson 1991). Deposition in these interior basins, beginning in the Early Cretaceous and peaking in the Albian (Box *et al.* 1984, Patton & Box 1989), overlaps with the inferred timing of uplift of source areas in the Brooks Range as dated by K–Ar ages of mica from the Schist Belt to the north and Ruby terrane to the south (Fig. 1a). Miller & Hudson (1991) argue that the crustal extension occurred during a discrete event that post-dated Jurassic to Early Cretaceous Brookian thrust faulting, as rapid subsidence and infilling of these basins coincides with inferred cessation of a major period of thrust faulting in the foreland of the Brooks Range (Mull 1979, 1982, 1985). This cessation is dated by the Albian Fortress Mountain Formation, which unconformably overlies strongly deformed Early Cretaceous and older rocks but is itself only gently folded (Mull 1982, 1985, Crowder 1987). An extensional interpretation of the greenschist-facies fabric in the south-central Brooks Range is most consistent with the Miller & Hudson (1991) model.

In the study area, $^{40}Ar/^{39}Ar$ step-heating experiments on seven separates of white mica from Schist Belt rocks yield disturbed spectra with individual step ages as old as 140 Ma and as young as 115 Ma (Lee *et al.* 1992, Miller *et al.* unpublished data). Total gas ages from these samples do not vary systematically with location or structural position in the section. Samples with older total gas ages yield convex-upward release profiles, and samples with younger ages yield flatter spectra. The significance of these ages and their variability across this region is still unclear. One possibility is that the micas represent more than one generation of metamorphic growth and/or

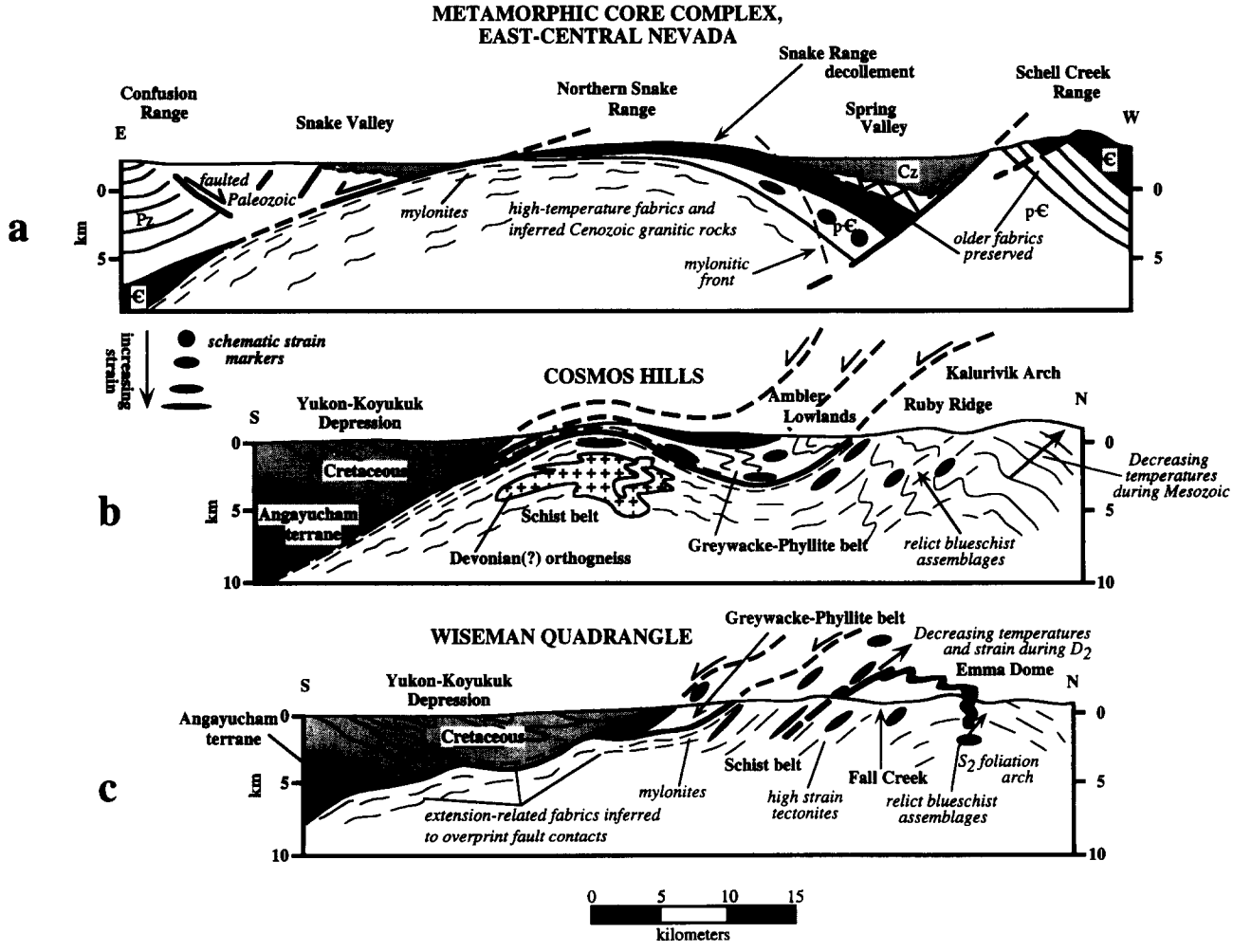

Fig. 9. Simplified cross-sections, all at the same scale, no vertical exaggeration, comparing structures developed along the southern flank of the Brooks Range to a well-studied core complex in the Basin and Range province. Snake Range cross-section modified from Gans & Miller (1985) with data from Lee *et al.* (1987). Cross-section of Cosmos Hills from Hitzman *et al.* (1982), Christiansen (1989) and Miller & Hudson (1991).

composition and preserve a variable component of older argon from incompletely degassed and reset M_1 micas, following the interpretation of similar data by Wijbrans & McDougall (1986). If so, 140 Ma is a minimum estimate for M_1 metamorphism, and the youngest dates provide a maximum age estimate for M_2. Alternatively, the disturbed spectra, which are similar to those obtained from equivalent metamorphic rocks on the Seward Peninsula, may be the result of incorporation of excess Ar during M_2 or younger times (e.g. Hannula *et al.* 1992), in which case the younger 115–120 Ma ages might represent a maximum age for D_2. These data are similar to those reported by Blythe *et al.* (in press) farther east who obtained variably disturbed spectra and total gas ages of 120–130 Ma on white mica separates.

SUMMARY AND CONCLUSIONS

Blueschist metamorphism in the internal zone of the Brooks Range fold and thrust belt probably developed during the Late Jurassic to Early Cretaceous phase of the Brookian orogeny, related to S-directed continental underthrusting and crustal thickening. High-P fabrics in the Brooks Range were widely retrogressed to greenschist-facies assemblages during the second metamorphic event (M_2). In the study area, relicts of M_1 blueschist-facies minerals are locally preserved as pseudomorphs. D_2 imprinted a widespread L–S tectonite fabric upon rocks of the Brooks Range Schist Belt. This D_2 fabric represents high strains as expressed by transposition of the older high-P foliation, formation of a down-dip stretching lineation, and local development of a mylonitic textures. In contrast to previous workers we interpret D_2, the dominant structural fabric in the Schist Belt, to result from extensional deformation within a down-to-the-south shear zone. Our conclusion is supported by microstructural kinematic indicators that are discussed in more detail in the companion to this paper.

The footwall of the Florence Creek fault consists of retrogressed blueschist of the Schist Belt. This brittle normal fault has been overprinted by down-to-the-south mylonitic fabrics of the shear zone. Near the structural top of the Schist Belt, quartzose rocks contain strongly asymmetric mylonitic textures. These are replaced by more symmetrical granoblastic textures with structural depth, suggesting that temperature-sensitive recovery processes dominated the textural development of quartz in deeper rocks, and that deformation became less rotational in that direction. D_2 L–S tectonites are pervasively developed at least 8 km northward into the Schist Belt. About 10 km north of the fault zone, D_2 strain decreases so that the older high-P fabric is not transposed and is better preserved. About 15 km north of the shear zone, the S_2 foliation is warped into a domal structure similar to the Wiseman arch farther east.

Extensional deformation along the southern flank of the Brooks Range shares important similarities in scale, geometry and nature to that of metamorphic core complexes of the Basin and Range province, U.S.A., but exhibits some important differences as well. The differences suggest that temperatures increased during the later stages of extension in the southern Brooks Range and adjacent Yukon–Koyukuk basin, allowing deformation and metamorphism of the normal faults themselves. This regional heating may be related to the intrusion of voluminous mid- to Late Cretaceous plutons immediately to the south of the study area. The exposure of structural levels inferred to be deeper than those exposed in the Basin and Range may be due to uplift and erosion related to later folding of the Brooks Range that accompanied Late Cretaceous to Tertiary crustal shortening in northern Alaska. This shortening is expressed by folding and thrust-faulting of the Cretaceous deposits of the Yukon–Koyukuk basin (Cushing & Gardner 1987), and possibly by the km-scale post-metamorphic folds in the Schist Belt, such as the Cosmos, Kalurivik and Wiseman arches.

The rocks in the Schist Belt we have studied were likely first metamorphosed under blueschist-facies conditions (Gottschalk 1987). Our results indicate that the dominant structural fabric in these rocks was imprinted during part of their exhumation history, under lower-P metamorphic conditions and probably higher geothermal gradients. Higher geothermal gradients may have been generated during Cretaceous magmatism that accompanied a regional phase of extension in Alaska (Miller & Hudson 1991). Final exhumation and exposure of these rocks was related to folding and erosion during a younger event of regional shortening. We emphasize that although we believe that regional extension was one of the causes involved in *final* exhumation of these rocks, none of the data reported here constrain the earlier part of the uplift path which may well have been by other mechanisms operating during crustal shortening.

Acknowledgements—This study was funded by a grant from ARCO Alaska, and made possible by helicopter and logistical support from the Trans-Alaska Crustal Transect Geologic Studies Project of the U.S. Geological Survey headed by T. E. Moore and W. J. Nokleberg. Final stages of the work were funded by NSF grant EAR 9018922. The Alaska Division of Geological and Geophysical Surveys loaned us aerial photographs, thin sections, and unpublished compilation maps of the late J. T. Dillon. These data and Dillon's pioneering work were vital prerequisites to this study. Important logistical assistance was provided by G. H. Pessel. Spirited discussions with H. G. Ave Lallement, P. P. Christiansen, R. R. Gottschalk, T. L. Hudson, T. E. Moore, C. G. Mull, W. J. Nokleberg, G. H. Pessel, R. R. Reifenstuhl, D. Solic and A. B. Till contributed to this study. Helpful comments by R. R. Gottschalk, J. W. Handschy and an anonymous reviewer improved the manuscript.

REFERENCES

Armstrong, R. L., Harakal, J. E., Forbes, R. B., Evans, B. W. & Thurston, S. P. 1986. Rb–Sr and K–Ar study of metamorphic rocks of the Seward Peninsula and southern Brooks Range, Alaska. In: *Blueschist and Eclogites* (edited by Evans, B. W. & Brown, E. H.). *Mem. geol. Soc. Am.* **164**, 185–203.

Ave Lallement, H. G., Oldow, J. S. & Gottschalk, R. R. 1989. Mesoscopic fault analysis in the south-central Brooks Range fold and thrust belt, Alaska. *Geol. Soc. Am. Abs. w. Prog.* **21**, 52.

Bell, T. H. & Johnson, S. E. 1989. Porphyroblast inclusion trails: The key to orogenesis. *J. metamorph. Geol.* **7**, 279–310.

Bell, T. H., Rubenbach, M. J. & Fleming, P. D. 1986. Porphyroblast nucleation, growth, and dissolution in regional metamorphic rocks as a function of deformation partitioning during foliation development. *J. metamorph. Geol.* **4**, 37–67.

Bird, K. J. 1977. Late Paleozoic carbonates from the south-central Brooks Range. *U.S. geol. Surv. Circ.* **751-B**, B19–B20.

Bishop, D. G. 1972. Progressive metamorphism from prehnite–pumpellyite to greenschist facies in the Dansey Pass area, Otago, New Zealand. *Bull. geol. Soc. Am.* **83**, 3177–3198.

Blythe, A. E., Bird, J. M. & Omar, G. I. In press. Constraints on the cooling history of the central Brooks Range, Alaska, from fission track and $^{40}Ar/^{39}Ar$ analyses. *Mem. geol. Soc. Am.*

Box, S. E. 1987. Late Cretaceous or younger SW-directed extensional faulting: Cosmos Hills, Brooks Range, Alaska. *Geol. Soc. Am. Abs. w. Prog.* **19**, 212.

Box, S. E., Patton, W. W. & Carlson, C. 1984. Early Cretaceous evolution of northeastern Yukon–Koyukuk Basin, west-central Alaska. *U.S. geol. Surv. Circ.* **967**, 21–24.

Brosge, W. P. & Reiser, H. N. 1964. Geologic map and section of the Chandalar quadrangle, Alaska: *U.S. geol. Surv. Misc. Geol. Invest. Map* **I-375**, scale 1:250 000.

Brosge, W. P. & Reiser, H. N. 1971. Preliminary bedrock geologic map: Wiseman and eastern Survey Pass quadrangles, Alaska. *U.S. geol. Surv. Open-file Map* **479**, scale 1:250 000.

Burchfiel, B. C., Zhiliang, C. K., Hodges, K. V., Yuping, L., Royden, L. H., Changrong, D. & Jiene, X. 1992. The South Tibetan detachment system, Himalayan orogen: extension contemporaneous with and parallel to shortening in a collisional mountain belt. *Spec. Pap. geol. Soc. Am.* **269**.

Christiansen, P. P. 1989. Structural, metamorphic and thermal evolution of the Cosmos Hills, northern Alaska. Unpublished M.S. thesis, Stanford University, California.

Crowder, K. 1987. Cretaceous basin to shelf transition in northern Alaska: Deposition of the Fortress Mountain Formation. In: *Alaska North Slope Geology, Pacific Section SEPM*, 449–458.

Cushing, G. W. & Gardner, M. C. 1987. The structural geology and tectonics of the central Yukon–Koyukuk Basin, western Alaska. *Geol. Soc. Am. Abst. w. Prog.* **19**, 633–634.

Dewey, J. F. 1988. Extensional collapse of orogens. *Tectonics* **7**, 1123–1139.

Dillon, J. T. 1989. Structure and stratigraphy of the southern Brooks Range and northern Koyukuk basin near the Dalton Highway. In: *Dalton Highway, Yukon River to Prudoe bay, Alaska, Bedrock Geology of the Eastern Koyukuk Basin, Central Brooks Range, and East-central Arctic Slope* (edited by Mull, C. G. & Adams, K. E.). *Dept Nat. Res. Alaska Div. Geol. Geophys. Surv. Guidebook* **7**, Vol. 2, 157–188.

Dillon, J. T., Brosge, W. P. & Dutro, J. T., Jr. 1986. Generalized geologic map of the Wiseman quadrangle, Alaska. *U.S. geol. Surv. Open-file Rep.* **OF 86-219**, scale 1:250 000.

Dillon, J. T., Hamilton, W. B. & Lueck, L. L. 1981. Geologic map of the Wiseman A-3 quadrangle, Alaska. *Alaska Div. Geol. Geophys. Surv. Open-file Rep.* **119**, 1 sheet, scale, 1:63 360.

Dillon, J. T., Pessel, G. H., Chen, G. H. & Veach, N. C. 1980. Middle Paleozoic magmatism and orogenesis in the Brooks Range, Alaska. *Geology* **8**, 338–343.

Dillon, J. T., Pessel, G. H., Lueck, L. L. & Hamilton, W. B. 1987. Geologic map of the Wiseman A-4 quadrangle, south-central Brooks Range, Alaska. *Alaska Div. Geol. Geophys. Surv. Prof. Rep.* **87**, 2 sheets, scale, 1:63 360.

Dillon, J. T., Solie, D. N., Decker, J. E., Murphy, J. M., Bakke, A. A. & Huber, J. A. 1989. Dalton Highway road log from South Fork Koyukuk River (Mile 156.2) to Chandalar Shelf (Mile 237.1). In: *Dalton Highway, Yukon River to Prudoe Bay, Alaska, Bedrock Geology of Eastern Koyukuk Basin, Central Brooks Range, and East-central Arctic Slope* (edited by Mull, C. G. & Adams, K. E.). *Alaska Dept Nat. Res. Div. Geol. Geophys. Surv. Guidebook* **7**, 74–100.

Dusel-Bacon, C., Brosge, W. P., Till, A. B., Fitch, M. R., Mayfield, C. F., Reiser, H. N. & Miller, T. P. 1989. Distribution, facies, ages and proposed tectonic associations of regionally metamorphosed rocks in northern Alaska. *Prof. Pap. U.S. geol. Surv.* **1497A**.

Gans, P. B. & Miller, E. L. 1985. Comment on the "Snake Range décollement interpreted as a major extensional shear zone" by J. M. Bartley and B. P. Wernicke. *Tectonics* **4**, 411–415.

Ghosh, S. K. & Sengupta, S. 1987. Progressive development of structures in a ductile shear zone. *J. Struct. Geol.* **9**, 277–287.

Gilbert, W. G., Wiltse, M. A., Carden, J. R., Forbes, R. B. & Hackett, S. W. 1977. Geology of Ruby Ridge, southwestern Brooks Range, Alaska. *Alaska Div. Geol. Geophys. Surv. Geol. Rep.* **51**.

Gottschalk, R. R. 1987. Structural and petrologic evolution of the south-central Brooks Range, Alaska. Unpublished Ph.D. dissertation, Rice University, Houston, Texas.

Gottschalk, R. R. 1990. Structural evolution of the Schist Belt, south-central Brooks Range fold and thrust belt, Alaska. *J. Struct. Geol.* **12**, 453–469.

Gottschalk, R. R. & Oldow, J. S. 1988. Low-angle normal faults in the south-central Brooks Range fold and thrust belt, Alaska. *Geology* **16**, 395–399.

Grantz, A., Moore, T. E. & Roeske, S. 1991. Continent–ocean transect A-3: Gulf of Alaska to Arctic Ocean. *Geol. Soc. Am. Centenniel Continent/Ocean Transect Ser.*, 3 sheets, scale 1:500 000.

Grybeck, D., Beikman, H. M., Brosge, W. P., Tailleur, I. L. & Mull, C. G. 1977. Geologic Map of the Brooks Range, Alaska. *U.S. geol. Surv. Open-file Map* **77-166,** scale 1:2 500 000.

Handschy, J. W. 1988. Sedimentology and structural geology of the Endicott Mountains allochthon, central Brooks Range, Alaska. Unpublished Ph.D. dissertation, Rice University, Houston, Texas.

Hannula, K. A., McWilliams, M. O. & Gans, P. B. 1992. ^{40}Ar–^{39}Ar and compositional data on white micas, Seward Peninsula, Alaska: Implications for the age of blueschist metamorphism. *Geol. Soc. Am. Abs. w. Prog.* **24**, 31.

Hitzman, M. W. 1984. Geology of the Cosmos Hills and its relationship to the Ruby Creek Copper-Cobalt deposit. Unpublished Ph.D. dissertation, Stanford University, California.

Hitzman, M. W., Proffet, J. M., Schmidt, S. & Smith T. E. 1986. Geology and mineralization of the Ambler District. *Econ. Geol.* **91**, 1592–1618.

Hitzman, M. W., Smith, T. E. & Proffet, J. M. 1982. Bedrock geology of the Ambler district, southwestern Brooks Range, Alaska. *Alaska Div. Geol. Geophys. Surv. Geol. Rep.* **75**, scale 1:125 000.

Hsu, K. J. 1992. Reply on "Exhumation of high-pressure metamorphic rocks". *Geology* **20**, 186.

Jones, D. L., Coney, P. J., Harms, T. A. & Dillon, J. T. 1988. Interpretive geologic map and supporting radiolarian data from the Angayucham terrane. Coldfoot area, southern Brooks Range, Alaska. *U.S. geol. Surv. Misc. Field Studies Map* **MF-1993**, scale 1:63 360.

Law, R. D., Miller, E., Little, T. A. & Lee, J. 1994. Extensional origin of ductile fabrics in the Schist Belt, Central Brooks Range, Alaska—II. Microstructural and petrofabric evidence. *J. Struct. Geol.* **16**.

Lee, J., Miller, E. L., Law, R. D. & Little, T. A. 1992. Metamorphic fabrics and sense-of-shear indicators in the southern Brooks Range "blueschist belt", Alaska. *Geol. Soc. Am. Abs. w. Prog.* **24**, 63.

Lee, J., Miller, E. L. & Sutter, J. F. 1987. Ductile strain and metamorphism in an extensional tectonic setting: a case study from the northern Snake Range, Nevada, U.S.A. In: Continental Extensional Tectonics (edited by Coward, M. P., Dewey, J. F. & Hancock, P. L.). *Spec. Publs geol. Soc. Lond.* **28**, 267–298.

Lister, G. S. & Snoke, A. W. 1984. S–C mylonites. *J. Struct. Geol.* **6**, 617–638.

McKenzie, D. 1978. Active tectonics of the Alpine–Himalayan belt: The Aegean Sea and surrounding regions. *Geophys. J. R. astr. Soc.* **55**, 217–254.

Mayfield, C. F., Tailleur, I. L. & Ellersieck, I. 1988. Stratigraphy, structure, and palinspastic syntheses of the western Brooks Range, northwestern Alaska. *Prof. Pap. U.S. geol. Surv.* **1399**, 143–186.

Miller, E. L. 1987. Dismemberment of the Brooks Range orogenic belt during middle Cretaceous extension. *Geol. Soc. Am. Abs. w. Prog.* **19**, 432.

Miller, E. L., Christiansen, P. P. & Little, T. A. 1990a. Structural studies in the southernmost Brooks Range, Alaska. *Geol. Ass. Can. Prog. w. Abs.* **15**, A–89.

Miller, E. L. & Hudson, T. L. 1991. Mid-Cretaceous extensional fragmentation of a Jurassic–Early Cretaceous compressional orogen, Alaska. *Tectonics* **10**, 781–796.

Miller, E. L. & Hudson, T. L. 1993. Reply: "Mid-Cretaceous extensional fragmentation of a Jurassic–Early Cretaceous compressional orogen, Alaska". *Tectonics* **12**, 1082–1086.

Miller, E. L., Law, R. D. & Little, T. A. 1990b. Evidence for extensional deformation on the southern flank of the Brooks Range in the Florence Creek area, Wiseman A-3 quadrangle, Alaska. *Geol. Soc. Am. Abs. w. Prog.* **22**, A183.

Moore, T. E., Wallace, W. K., Bird, K. J., Karl, S. M., Mull, C. G. & Dillon, J. T. 1992. Stratigraphy, structure and geologic synthesis of northern Alaska. *U.S. geol. Surv. Open-file Rep.* **92-330**.

Mull, C. G. 1979. Nanushuk Group deposition and the late Mesozoic structural evolution of the central and western Brooks Range and Arctic slope. *U.S. geol. Surv. Circ.* **794**, 5–13.

Mull, C. G. 1982. Tectonic evolution and structural style of the Brooks

Range, Alaska: An illustrated summary. In: *Geologic Studies of the Cordilleran Thrust Belt* (edited by Blake, R. B.). Rocky Mountain Association of Geologists, Denver, 1–45.

Mull, C. G. 1985. Cretaceous tectonics, depositional cycles, and the Nanushuk Group, Brooks Range and Arctic Slope, Alaska. In: *Geology of the Nanushuk Group and Related Rocks, North Slope, Alaska* (edited by Ahlbrandt, T. S.). *Bull. U.S. geol Surv.* **1614**, 7–36.

Mull, C. G., Roeder, D. H., Tailleur, I. L., Pessel, G. H., Grantz, A. & May, S. D. 1987. Geologic sections and maps across Brooks Range and Arctic slope to Beaufort Sea, Alaska. *Geol. Soc. Am. Map & Chart Ser.* **MC-28S**.

Murphy, J. M. & Patton, W. W. 1988. Geologic setting and petrography of the phyllite and metagraywacke thrust panel, north-central Alaska. *U.S. geol. Surv. Circ.* **1016**, 104–108.

Murphy, J. M., O'Sullivan, P. B., Nelson, S., Miller, E. L. & Moore, T. E. 1991. Apatite fission track thermochronology of the southern Brooks Range, Alaska: Evidence of episodic Tertiary uplift, segmentation and high-angle fault reactivation. *Eos* **72**, 299.

Nelson, S. W. & Grybeck, D. 1980. Metamorphic rocks of the Survey Pass quadrangle, Brooks Range Alaska. *U.S. geol. Surv. Misc. Field Studies Map* **MF 1176-C**, scale 1:250 000.

Oldow, J. S., Ave Lallement, H. G. & Gottschalk, R. R. 1991. Timing and kinematics of Cretaceous contraction and extension in the southern Brooks Range, Alaska. *Geol. Soc. Am. Abs. w. Prog.* **23**, 85.

Oldow, J. S., Bally, A. W., Ave Lallement, H. G. & Leeman, W. P. 1989. Phanerozoic evolution of the North American Cordillera; United States and Canada. In: *The Geology of North America—An Overview* (edited by Bally, A. W. & Palmer, A. R.). Geological Society of America, Boulder, Colorado, 139–232.

Oldow, J. S., Seidensticker, C. M., Phelps, J. C., Julian, F. E., Gottschalk, R. R., Boler, K. W., Handschy, J. W. & Ave Lallement, H. G. 1987. Balanced cross-sections through the central Brooks Range and North Slope, Arctic Alaska. Eight plates, American Association of Petroleum Geologists, Tulsa, Okla.

Passchier, C. W. & Simpson, C. 1986. Porphyroclast systems as kinematic indicators. *J. Struct. Geol.* **8**, 831–843.

Patrick, B. E., Dinklage, W. S. & Till, A. B. 1991. Metamorphism and progressive deformation in the Walker Lake region of the southern Brooks Range, Alaska. *Geol. Soc. Am. Abs. w. Prog.* **23**, 87.

Patrick, B., Till, A. B. & Dinklage, W. S. In press. An inverted metamorphic field gradient in the central Brooks Range, Alaska, and implications for exhumation of high pressure/low temperature metamorphic rocks. *Lithos*.

Patton, W. W., Jr & Box, S. E. 1989. Tectonic setting of the Yukon–Koyukuk basin and its borderlands, western Alaska. *J. geophys. Res.* **94**, 15 807–15 820.

Platt, J. P. 1983. Progressive refolding in ductile shear zones. *J. Struct. Geol.* **5**, 619–622.

Platt, J. P. 1986. Dynamics of orogenic wedges and the uplift of high-pressure metamorphic rocks. *Bull. geol. Soc. Am.* **97**, 1037–1053.

Platt, J. P. 1992. Comment on "Exhumation of high-pressure metamorphic rocks". *Geology* **20**, 186–187.

Platt, J. P. & Vissers, R. L. M. 1980. Extensional structures in anisotropic rocks. *J. Struct. Geol.* **2**, 397–410.

Ramsay, J. G., Casey, M. & Kligfield, R. 1983. Role of shear in development of the Helvetic fold and thrust belt of Switzerland. *Geology* **11**, 439–442.

Ramsay, J. G. & Huber, M. I. 1983. *The Techniques of Modern Structural Geology, Volume* 1: *Strain Analysis*. London, Academic Press.

Roeder, D. & Mull, C. G. 1978. Tectonics of the Brooks Range ophiolites, Alaska. *Bull. Am. Ass. Petrol. Geol.* **62**, 1696–1713.

Sanderson, D. J. 1973. The development of fold axes oblique to the regional trend. Tectonophysics **16**, 55–70.

Silberling, N. J. & Jones, D. L. 1984. Lithotectonic terrane maps of the North American Cordillera. *U.S. geol. Surv. Open-file Rep.* **OFR 84-523**.

Till, A. B., Box, S. E., Roeske, S. M. & Patton, W. W. 1993. Comment on "Mid-Cretaceous fragmentation of a Jurassic–Early Cretaceous compressional orogen, Alaska" by E. L. Miller and T. L. Hudson. *Tectonics* **12**, 1076–1081.

Till, A. B., Schmidt, J. M. & Nelson, S. W. 1988. Thrust involvement in metamorphic rocks, southwestern Brooks Range, Alaska. *Geology*, **16**, 930–933.

Till, A. B. & Moore, T. E. 1991. Tectonic relations of the schist belt, southern Brooks Range, Alaska. *Eos* **72**, 295.

Tobish, O. T. & Paterson, S. R. 1988. Analysis and interpretation of composite foliations in areas of progressive deformation. *J. Struct. Geol.* **10**, 745–754.

Wijbrans, J. & McDougall, I. 1986. $^{50}Ar/^{39}Ar$ dating of white micas from an Alpine high-pressure metamorphic belt on Naxos (Greece): the resetting of the argon isotopic system. *Cont. Miner. Petrol.* **93**, 187–194.

Wilber, S. C., Siok, J. P. & Mull, C. G. 1987. A comparison of two petrographic suites of the Okpikruak Formation: A point-count analysis. In: *Alaskan North Slope Geology, Volume* 1 (edited by Tailleur, I. & Weimer, P.). *Spec. Publs. Pacific Section, Soc. econ. Paleont. Miner. Bakersfield, Calif.* 441–447.

Williams, P. F. & Price, G. P. 1990. Origin of kink-bands and shear-band cleavage in shear zones. *J. Struct. Geol.* **12**, 145–164.